

## ORIGINAL ARTICLE

## A novel oncogenic BTK isoform is overexpressed in colon cancers and required for RAS-mediated transformation

E Grassilli<sup>1,2</sup>, F Pisano<sup>1,2</sup>, A Cialdella<sup>1,2</sup>, S Bonomo<sup>1</sup>, C Missaglia<sup>1</sup>, MG Cerrito<sup>1</sup>, L Masiero<sup>1</sup>, L Ianzano<sup>1</sup>, F Giordano<sup>1</sup>, V Cicirelli<sup>1</sup>, R Narloch<sup>1</sup>, F D'Amato<sup>3</sup>, B Noli<sup>3</sup>, GL Ferri<sup>3</sup>, BE Leone<sup>1</sup>, G Stanta<sup>4</sup>, S Bonin<sup>4</sup>, K Helin<sup>5,6,7</sup>, R Giovannoni<sup>1</sup> and M Lavitrano<sup>1</sup>

Bruton's tyrosine kinase (BTK) is essential for B-cell proliferation/differentiation and it is generally believed that its expression and function are limited to bone marrow-derived cells. Here, we report the identification and characterization of p65BTK, a novel isoform abundantly expressed in colon carcinoma cell lines and tumour tissue samples. p65BTK protein is expressed, through heterogeneous nuclear ribonucleoprotein K (hnRNPK)-dependent and internal ribosome entry site-driven translation, from a transcript containing an alternative first exon in the 5'-untranslated region, and is post-transcriptionally regulated, via hnRNPK, by the mitogen-activated protein kinase (MAPK) pathway. p65BTK is endowed with strong transforming activity that depends on active signal-regulated protein kinases-1/2 (ERK1/2) and its inhibition abolishes RAS transforming activity. Accordingly, p65BTK overexpression in colon cancer tissues correlates with ERK1/2 activation. Moreover, p65BTK inhibition affects growth and survival of colon cancer cells. Our data reveal that BTK, via p65BTK expression, is a novel and powerful oncogene acting downstream of the RAS/MAPK pathway and suggest that its targeting may be a promising therapeutic approach.

*Oncogene* advance online publication, 25 January 2016; doi:10.1038/onc.2015.504

## INTRODUCTION

Bruton's tyrosine kinase (BTK) is a nonreceptor tyrosine kinase initially identified as the defective protein in human X-linked agammaglobulinemia.<sup>1</sup> Since its discovery, BTK has been considered a tissue-specific protein, being expressed throughout the hematopoietic compartment, except T cells and plasma cells. BTK plays a critical role in several hematopoietic signalling pathways including those mediated by several chemokine receptors and the B-cell antigen receptor.<sup>2</sup> In B lymphocytes, as an essential component of the B-cell signalosome, BTK is involved in transducing activation, proliferation, maturation, differentiation and survival signals and is an upstream activator of multiple anti-apoptotic signalling molecules and networks, such as signal transducer and activator of transcription 5, nuclear factor- $\kappa$ B and the phosphatidylinositol-3-kinase/AKT/mammalian target of rapamycin pathway.<sup>3</sup> BTK is overexpressed in several B-cell malignancies<sup>3</sup> and different kinase-defective isoforms, exerting a dominant-negative effect over full-length BTK, have been reported in B-cell precursor leukaemia cells.<sup>4</sup> Despite that its hyperactivation plays a pivotal role in chronic B-cell receptor signalling required for the survival of neoplastic B cells and that in experimental settings gain-of-function mutations providing BTK with transforming potential have been described,<sup>2,5–7</sup> no constitutively active BTK mutants have been identified so far in hematopoietic neoplasias, thus leaving the oncogenicity of BTK an open question. BTK has emerged as a new molecular target for the treatment of B-lineage leukaemias and lymphomas, and ibrutinib is the first BTK-specific inhibitor that entered the clinic, having been recently approved for the treatment of mantle cell

lymphoma and chronic lymphocytic leukaemia. Moreover, ibrutinib and other BTK inhibitors are in advanced clinical trials for other hematological malignancies.<sup>3</sup>

Here, we report the identification of p65BTK, a novel BTK isoform, and show that it is expressed in colon cancers and that its expression is regulated by its 5'-untranslated region (UTR) via mitogen-activated protein kinase (MAPK)/heterogeneous nuclear ribonucleoprotein K (hnRNPK)-dependent and internal ribosome entry site (IRES)-driven translation of an alternatively spliced mRNA. Moreover, we demonstrate that p65BTK is a novel and powerful oncoprotein acting downstream of the RAS/MAPK pathway and a mediator of RAS-induced transformation.

## RESULTS

p65BTK is widely expressed in colon carcinoma cell lines and tissues

Preliminary data from our laboratory indicated that, unexpectedly, BTK is expressed in colon carcinoma cells, and thus we sought to define its function in colonic tissue. First, we observed that BTK is abundantly expressed in all colon cancer cell lines and tumour tissues analysed (Figures 1a and b). While studying the expression of BTK we noticed that its apparent molecular weight on SDS-polyacrylamide gel electrophoresis was lower than expected (Figure 1c). The downregulation of BTK expression by using specific small interfering RNA (siRNA) confirmed that the lower band is encoded by the *BTK* gene (Figure 1d). As alternative splicing of *BTK* mRNA has been reported in B-cell malignancies,<sup>4</sup> we set out to identify the isoform expressed in colon cancers.

<sup>1</sup>School of Medicine and Surgery, University of Milano-Bicocca, Monza, Italy; <sup>2</sup>BiOnSil srl, Monza, Italy; <sup>3</sup>NEF-Laboratory, Department of Biomedical Science, University of Cagliari, Monserrato, Italy; <sup>4</sup>Department of Medical Sciences, University of Trieste, Cattinara Hospital, Trieste, Italy; <sup>5</sup>Biotech Research and Innovation Centre (BRIC), University of Copenhagen, Copenhagen, Denmark; <sup>6</sup>Center for Epigenetics, University of Copenhagen, Copenhagen, Denmark and <sup>7</sup>Danish Stem Cell Center (Danstem), University of Copenhagen, Copenhagen, Denmark. Correspondence: Professor E Grassilli or Professor M Lavitrano, School of Medicine and Surgery, University of Milano-Bicocca, Via Cadore 48, Monza, MB 20900, Italy.

E-mail: emanuela.grassilli@unimib.it or marialuisa.lavitrano@unimib.it

Received 20 May 2015; revised 7 December 2015; accepted 7 December 2015

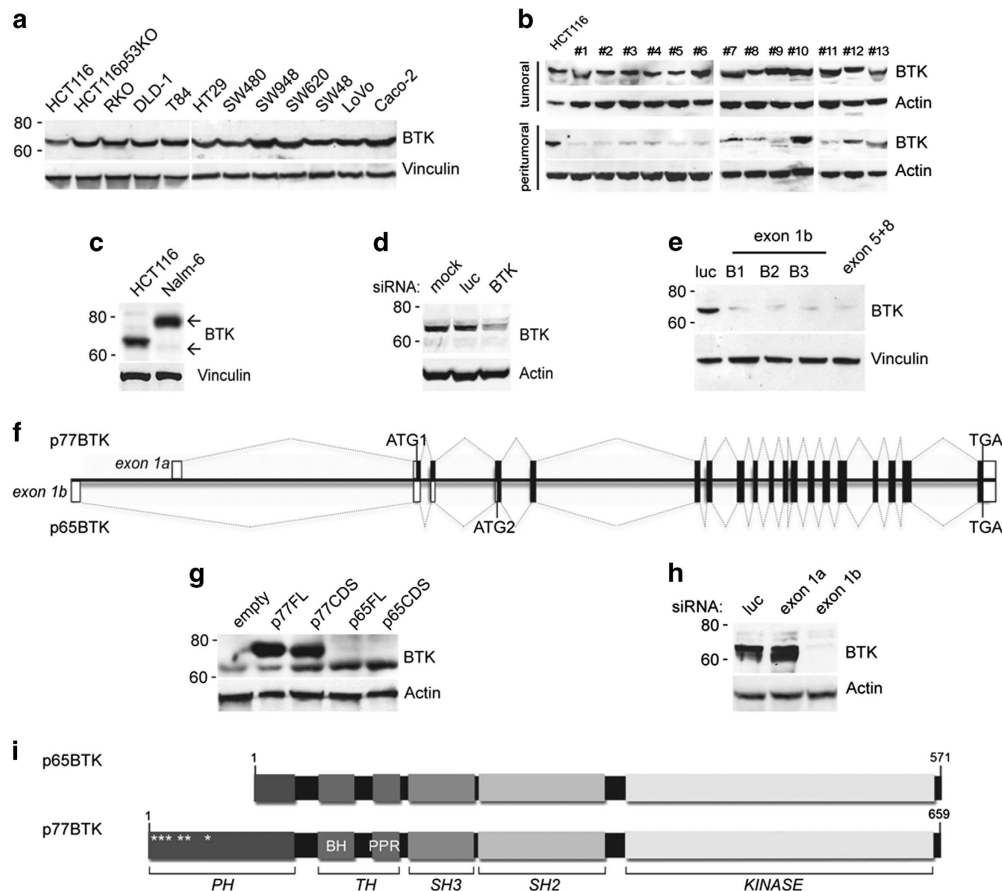


**Figure 1.** p65BTK, a novel isoform of Bruton's tyrosine kinase, is widely expressed in colon carcinoma cell lines and tissues. **(a, b)** BTK expression in colon cancer cell lines **(a)** or patients' biopsy **(b)** lysates. Western blots probed with a commercial BTK antibody (Santa Cruz, sc-1696). **(c)** Western blot showing that in colon carcinoma cells (HCT116) BTK has a lower molecular weight than in lymphoid leukaemia (Nalm-6). **(d)** Western blot of BTK expression in HCT116 cells after silencing with BTK-specific siRNA (exons 5+8). **(e)** Western blot of BTK expression in HCT116 cells upon silencing using exon 1b (B1–3)-targeting siRNAs. **(f)** *BTK* gene and mRNAs encoding p77BTK and p65BTK. ATG1 and ATG2: start codons, black/white boxes: translated/untranslated exons. Exon 1a and exon 1b are indicated. **(g)** BTK expression in 293T cells transiently transfected with empty vector (empty) and plasmids encoding p77BTK or p65BTK coding sequence (p77CDS, p65CDS), p77BTK CDS or p65BTK CDS full lengths (p77FL, p65FL). **(h)** Western blot of p65BTK expression in 293T cells transiently transfected with p65FL plasmid followed by silencing with exon1b-specific siRNAs. **(i)** p65 and p77 BTK protein organization: PH domain. BH, BTK homology region; PPR, PolyProline region; TH, Tec homology domain; \*phosphoinositide binding site.

Using a PCR strategy covering the entire coding sequence (CDS) of *BTK*, we were unable to amplify the 5' of the mRNA expressed in colon cells (Supplementary Figures S1a and b). Indeed, 5'RACE (rapid amplification of cDNA ends)/sequencing experiments on colon cancer cell line-derived complementary DNAs (cDNAs) followed by ClustalW alignment (<http://www.clustal.org/clustal2/>) (Supplementary Figures S1c and d) revealed that colon cancer-derived mRNA contains a first exon different from the one expressed in B cells. Moreover, BLAST alignment showed that the 300 bp long exon mapped 15 192 bp upstream of the first known *BTK* exon (Supplementary Figure S1e). We named the exon '1b', whereas the known exon 1 was referred to as 'exon 1a'. By using isoform-specific siRNAs (Figure 1e) we confirmed that the BTK expressed in colon cancer cells is translated from exon 1b-containing mRNA and, because of its apparent molecular weight, we named it p65BTK. Analysis of p65BTK cDNA with an open reading frame (ORF) predicting program<sup>8</sup> revealed—beside the expected starting codon in exon 2 (ATG1)—a putative start codon in exon 4 (Figure 1f) whose usage would lead to a predicted protein of ≈65 kDa. Transfection of 293T cells with a plasmid expressing either a putative CDS starting from the ATG in exon 4 (ATG2) or the full-length cDNA led to the expression of ≈65-kDa BTK (Figure 1g). Accordingly, siRNAs targeting exon 1b, but not

those targeting exon 1a, specifically abolished the synthesis of 65 kDa isoform in overexpressing 293T cells (Figure 1h). Compared with the previously known isoforms, the predicted p65BTK protein would lack most of the N-terminal Pleckstrin homology (PH) domain (Figure 1h). To study the expression of the novel BTK isoform we then raised and characterized BN49 polyclonal antibody specific for p65BTK (Supplementary Figures S1f and g).

hnRNPK and active ERKs post-transcriptionally regulate p65BTK expression

To further demonstrate p65BTK production from the identified RNA we performed *in vitro* translation assays using a plasmid containing p65BTK full-length cDNA. Surprisingly, in this setting the protein was not translated, whereas small amounts of p65BTK were obtained using a plasmid bearing either wild-type p77BTK full-length cDNA or its mutated counterpart with a missense mutation in the starting codon for 77 kDa BTK (ATG1) (Figure 2a). Hence, within the context of p77BTK mRNA, the ATG2 can also be recognized as a starting codon, although with much lower efficiency.

The lack of p65BTK expression in cell-free systems, together with the observation that the high levels of protein expression in cancer tissues (Figure 1b) were not mirrored by increases of

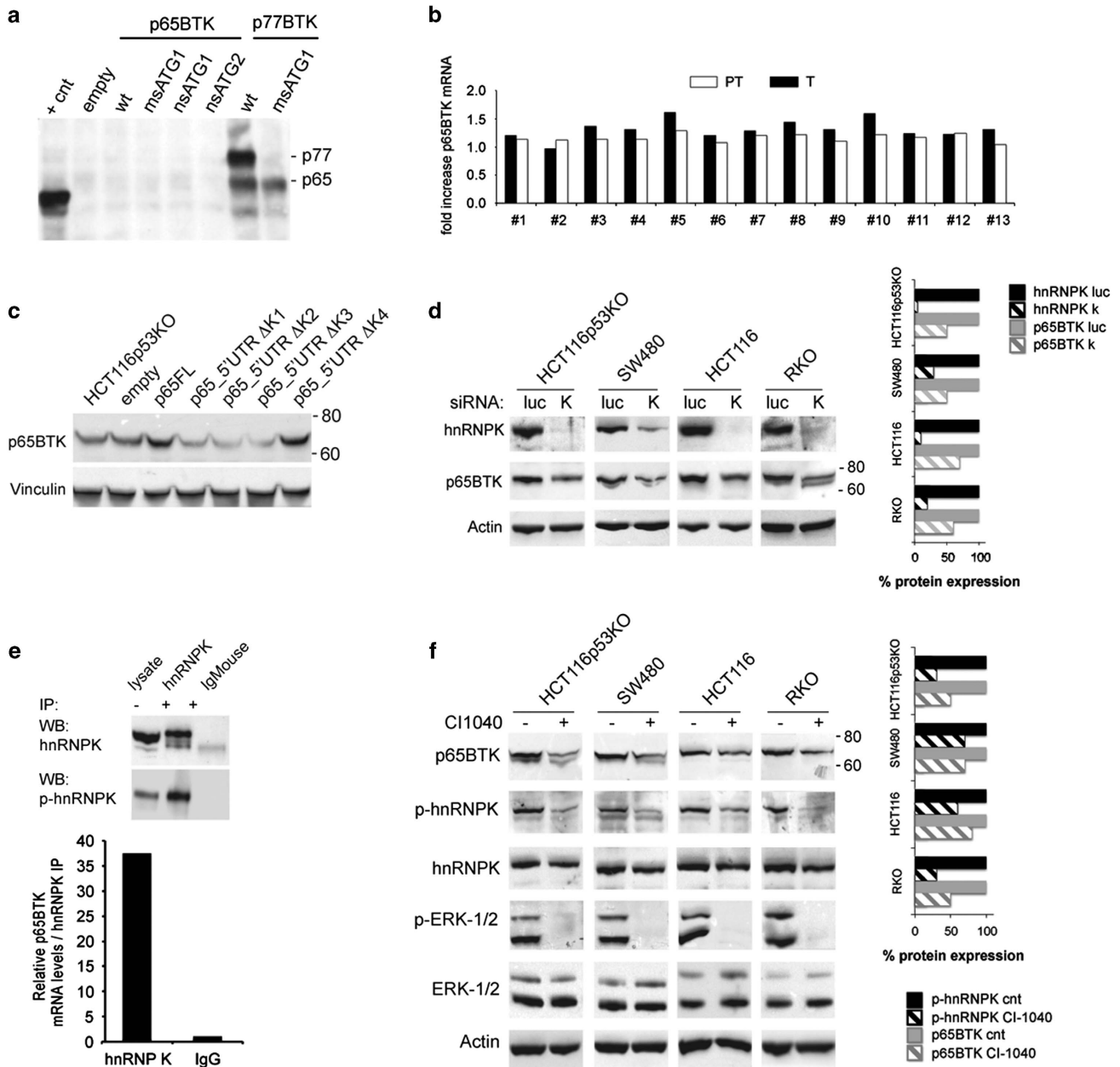


**Figure 2.** hnRNPK and active ERKs post-transcriptionally regulate p65BTK expression. **(a)** *In vitro* translation assay performed with the following plasmids: empty vector (empty); p65FL (wt), p65\_msATG1, p65\_nsATG1, p65\_nsATG2, p77\_5'UTR or p77\_msATG1. +cnt indicates the positive control included in the commercial kit used for the reaction. **(b)** p65BTK mRNA expression in matched samples of tumoural and peritumoural colon tissue from CRC patients (same patients as in Figure 1b). mRNA was quantified by Taqman assay and expression levels normalized to phosphoglycerate kinase. **(c)** Western blot of 293T cells transfected with empty vector (empty) or the following plasmids: p65FL, p65\_5'UTRΔK1, p65\_5'UTRΔK2, p65\_5'UTRΔK3, p65\_5'UTRΔK4. Deletion of all four binding sites allowed p65BTK overexpression most likely by rendering the transcript as it would be a CDS. **(d)** Western blot of p65BTK levels in colon cancer cell lines after siRNA-mediated depletion of hnRNPK (K). Transfection with siRNAs targeting luciferase (luc) was used as a control. On the right, the percentage of hnRNPK and p65BTK protein expression of each sample as calculated and normalized to actin by ImageJ program (<http://imagej.nih.gov/ij/>). **(e)** (top) Anti-hnRNPK and anti-phospho-hnRNPK western blots after RNA immunoprecipitation using anti-hnRNPK and isotype-matched control (Ig mouse) antibodies. **(e)** (bottom) Real-time PCR of p65BTK mRNA recovered by RIP in hnRNPK and IgG immunoprecipitates. **(f)** Western blot of p65BTK expression and hnRNPK-Ser284 phosphorylation following ERK1/2 inhibition with the MEK1/2 inhibitor CI-1040 (10 μM). Levels of total and phospho-ERKs are also shown. Cell lysates were obtained 24 h after CI-1040 addition but for HCT116p53KO cells, where p65BTK reduction is most prominent, at 16 h. On the right, the percentage of p-hnRNPK and p65BTK protein expression of each sample was calculated and normalized to actin by ImageJ program.

p65BTK mRNA expression in the same tissues (Figure 2b), led us to hypothesize a post-transcriptional regulation mediated by a cellular protein binding to the 5'UTR to promote the translation of exon 1b-containing mRNA. Indeed, analysis of the 5'UTR revealed the presence of four putative hnRNPK binding sites and

three upstream ORFs<sup>9</sup> (Supplementary Figure S2a). hnRNPK is a RNA-binding nuclear protein involved in chromatin remodelling, transcription, splicing, translation and mRNA stability,<sup>10</sup> over-expressed and aberrantly localized in the cytoplasm in colorectal cancers.<sup>11</sup> Indeed, transfecting p65BTK-encoding plasmids

progressively deleted of the hnRNPK binding sites hampered its overexpression (Figure 2c). Moreover, p65BTK expression in colon cancer cells decreased upon silencing of hnRNPK by RNA interference (Figure 2d).

Analysis of p65BTK 5'UTR by a RNA structure prediction software (Supplementary Figure S2b) revealed a complex folding pattern, with the ATG1 hidden in a hairpin loop. We therefore hypothesized that 5'UTR-bound hnRNPK would promote a three-dimensional structure favouring the ribosome to start the translation from ATG2.

We then performed RNA immunoprecipitation (RIP) experiments to confirm the direct interaction of hnRNPK with p65BTK-encoding mRNA (Figure 2e). Previous results have shown that signal-regulated protein kinase-1/2 (ERK1/2)-mediated Ser284 phosphorylation leads to the relocalization of hnRNPK from the nucleus to the cytoplasm, where it accumulates<sup>12</sup> and increases MYC mRNA translation.<sup>13</sup> Interestingly, we also showed that hnRNPK (bound to p65BTK-encoding mRNA) is phosphorylated (Figure 2e), and we therefore investigated whether ERK1/2 might regulate p65BTK expression. As shown in Figure 2f, ERK1/2 inhibition (by MEK1/2 inhibitor CI-1040) indeed led to the decrease of both hnRNPK-Ser284 phosphorylation and p65BTK.

Taken together, these results demonstrate that p65BTK levels are regulated by both hnRNPK and active ERK1/2.

hnRNPK post-transcriptionally regulates p65BTK expression via IRES-dependent translation of exon 1b-containing mRNA

The presence of several ORFs in the 5'UTR of p65BTK together with the fact that MYC translation in leukemic cells is hnRNPK dependent and IRES mediated<sup>13</sup> led us to investigate whether p65BTK translation is also driven by an IRES. We identified a putative IRES in the 5'UTR of p65BTK mRNA (Supplementary Figures S3a and b) and showed that eIF4G2, a translation initiation factor involved in IRES-mediated translation,<sup>14</sup> co-immunoprecipitates with hnRNPK and p65BTK-encoding mRNA (Figure 3a). Next, we verified the presence of an IRES in the 5'UTR by demonstrating green fluorescent protein (GFP) expression following transfection of HeLa cells with a bicistronic vector in which GFP translation is under the control of p65BTK 5' UTR (Figure 3b). Accordingly, GFP expression increased when the experiment was repeated in the presence of 200 nM Rapamycin—which blocks cap-dependent translation and stimulates IRES-mediated translation<sup>15</sup>—and was abolished by 200 nM Cymarin—a cardiac glycoside recently identified as a potent inhibitor of MYC IRES-mediated translation<sup>16</sup> (Figure 3b). The presence of a cryptic promoter was ruled out by showing that a unique transcript coding for both red fluorescent protein (RFP) and GFP is transcribed in transfected cells (Supplementary Figure S3c). Finally, IRES-mediated translation of endogenous p65BTK was confirmed by demonstrating a time-dependent increase and decrease of p65BTK levels on treatment of colon cancer cells with Rapamycin and Cymarin, respectively (Figure 3c). Notably, in reporter assay we also demonstrated that hnRNPK is required for IRES-mediated translation of GFP, as its depletion by siRNA (Figure 3d) as well as the deletion of all hnRNPK binding sites (Supplementary Figure S4), completely abolished GFP expression.

Altogether, these data demonstrate that IRES-mediated translation of p65BTK mRNA strictly depends on hnRNPK.

p65BTK is a novel oncogenic protein acting downstream of RAS/ERK pathway and is overexpressed in colon cancers

In view of the abundant expression of p65BTK in colon carcinomas and its IRES-mediated translation,<sup>17</sup> we suspected that p65BTK could have oncogenic properties. Indeed, transfection of a plasmid encoding full-length p65BTK (Figures 4a–d) transformed NIH3T3 fibroblasts, whereas p77BTK overexpression did not

(Figure 4d). Notably, p65BTK was more potent than H-RASV12, used as a positive control, inducing more and larger colonies and foci. Inhibition of p65BTK-mediated transformation by use of the specific BTK inhibitor Ibrutinib<sup>3,18,19</sup> indicated that p65BTK oncogenic capacity is dependent on its kinase activity. Moreover, Ibrutinib addition also blocked H-RASV12-mediated transformation (Figure 4d). Interestingly, we found that BTK overexpression in NIH3T3 cells induced high levels of endogenous RAS (Figure 4a). Even though wild-type RAS overexpression is not transforming,<sup>20–23</sup> its expression appeared necessary for p65BTK-mediated transformation, as the RAS inhibitor FTI277, as well as cotransfection with a RAS-DN plasmid, abolished p65BTK-mediated transformation of NIH3T3 cells (Figure 4d and Supplementary Figure S5b). Conversely, H-RASV12 overexpression increased endogenous p65BTK (Figure 4a) and endogenous RAS knockdown rapidly depleted p65BTK (Supplementary Figure S5a), confirming that RAS indeed regulates p65BTK expression. However, p65BTK silencing did not affect endogenous RAS expression (Supplementary Figure S5a), suggesting that the observed endogenous RAS induction in p65BTK-transfected NIH3T3 cells is an effect of exogenous p65BTK overexpression. Finally, p65BTK-mediated transformation was suppressed when blocking RAS/MAPK pathway downstream of RAS, namely by using MEK1/2-inhibitor CI-1040 (Figure 4d). Altogether, these data indicate that p65BTK is an obligate effector of activated RAS.

We then confirmed our results showing that p65BTK expression parallels ERK1/2 activation and abnormal hnRNPK cytoplasmic localization by immunohistochemical analysis on paired peritumoural/tumoural samples from the same 13 colon carcinoma patients whose tissues have already been analysed for p65BTK expression in Figures 1b and 2b (Figure 4e, Supplementary Figure S6 and Supplementary Table S1).

Furthermore, we analysed p65BTK expression in a cohort of 83 stage II colon carcinoma patients and found that in 68.7% of peritumoural/tumoural sample pairs, p65BTK was more expressed in tumoural than in peritumoural tissue (Figure 4f); in addition, the grading of p65BTK according to an increasing intensity of the staining in tumoural samples (Supplementary Figure S7) showed moderate to high levels of the protein in the 74.7% of colon cancer tissues analysed (Figure 4g).

Taken together, our results suggest that p65BTK is an oncoprotein whose expression and transforming activity are tightly controlled, via hnRNPK, by the RAS/ERK pathway and that p65BTK overexpression in colon carcinomas reflects hyperactivation of the RAS/ERK pathway.

p65BTK inhibition affects growth and survival of colon cancer cells  
Finally, we tested the requirement of p65BTK in colon cancer cell biology. For all colon cancer cell lines tested, *in vitro* dose–response experiments showed that concentrations up to 10  $\mu$ M Ibrutinib caused a slight to moderate decrease in proliferation in the short term (Figure 5a) and strongly affected clonogenicity in the long term (Figure 5b); higher doses further inhibited the proliferation of all cell lines and completely suppressed cell growth at 30  $\mu$ M (Figures 5a and c) concomitantly with a significant increase of cell death (Supplementary Figure S8a). Similar results were obtained treating colon cancer cell lines with AVL-292, a different BTK inhibitor also in clinical trials for treating B-cell malignancies.<sup>19</sup> Notably, AVL-292 at 10  $\mu$ M almost completely suppressed cell growth and had a mild but significant cytotoxic effect (Supplementary Figure S8b) that increased in a dose-dependent manner (Supplementary Figure S8c).

## DISCUSSION

Since its discovery, BTK has been considered a tissue-specific kinase expressed only in bone marrow-derived cells.<sup>2</sup> In particular,

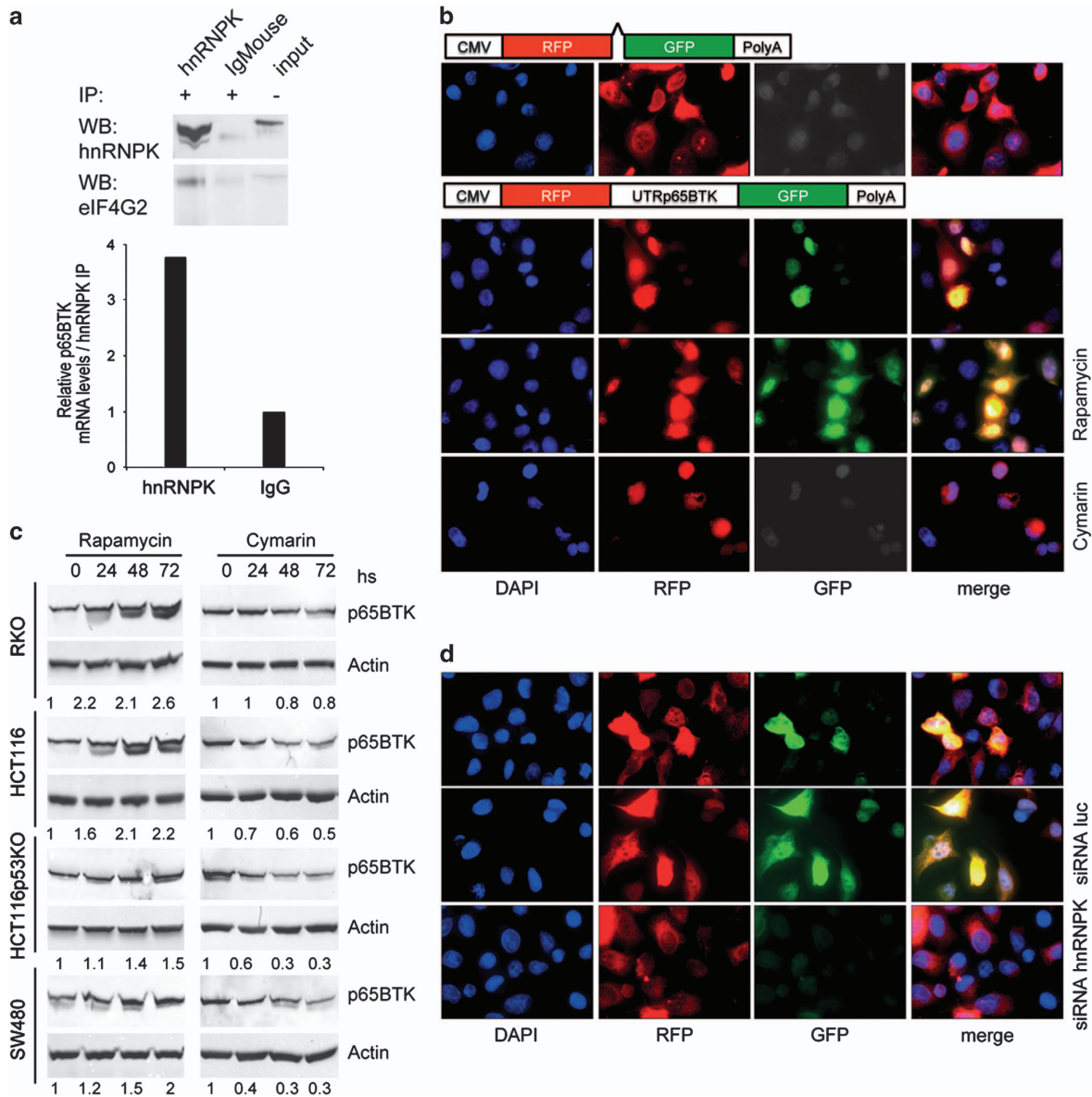


**Figure 3.** hnRNPk post-transcriptionally regulates p65BTK expression via IRES-dependent translation of exon 1b-containing mRNA. **(a)** Anti-hnRNPk antibodies immunoprecipitate a complex containing hnRNPk, eIF4G2 (top) and p65BTK mRNA (bottom) from HCT116p53KO lysates. **(b)** Fluorescence of HeLa cells transfected with a bicistronic vector encoding RFP under the control of CMV promoter and GFP not preceded by a regulatory region (first row) or under the control of p65BTK 5'UTR (second to fourth row) and left untreated (second row) or treated with Rapamycin 200 nM (third row) or Cymarin 100 nM (fourth row) for 36 h. DAPI was used to stain nuclei. **(c)** Time-dependent variation of p65BTK expression after treatment of colon cancer cells with 200 nM Rapamycin (left) and 200 nM Cymarin (right). Fold variation of p65BTK protein expression of each sample was calculated and normalized to actin by ImageJ program. **(d)** HeLa cells were transfected with the same bicistronic reporter as in **(b)** and luc-targeted siRNAs (second row) or hnRNPk-targeted siRNAs (third row). DAPI was used to stain nuclei.

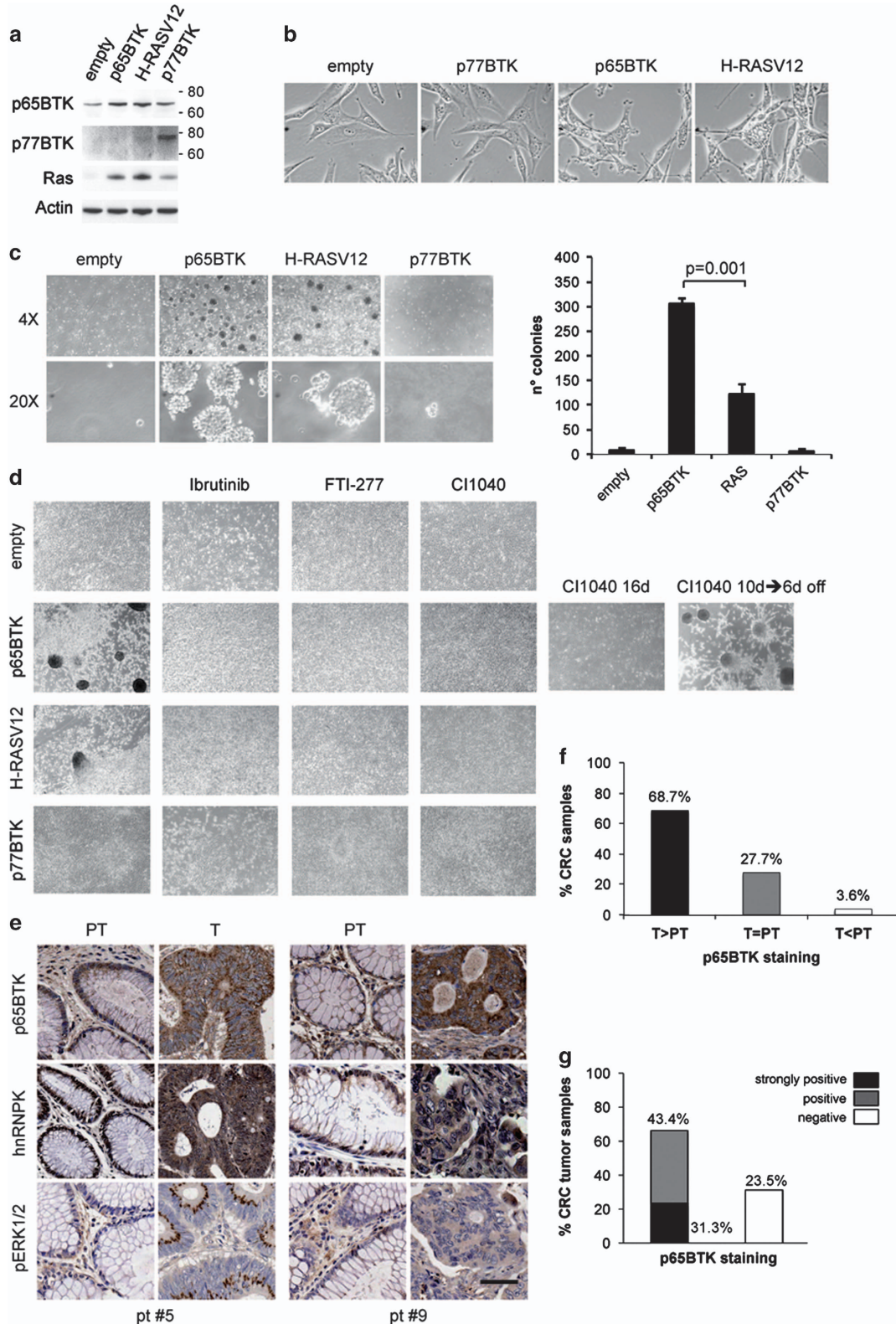
BTK transduces essential signals for the proliferation and differentiation of B lymphocytes and it has been found over-expressed/constitutively active in several B-lineage lymphoid malignancies.<sup>3</sup> Here we report the identification and characterization of p65BTK, a novel oncogenic isoform, whose 5'UTR-regulated expression is finely tuned downstream of ERK1/2 activation via hnRNPk- and IRES-dependent translation, whose activity is required for H-RASV12-induced transformation and whose levels are increased in a high percentage of colon cancers.

The most striking finding of this paper is that not only is BTK expressed outside of the hematopoietic compartment but, via p65BTK expression, is also a potent oncogene. Different kinase-defective isoforms of BTK have been reported in B-cell precursor

leukaemia cells,<sup>4</sup> and an 80-kDa isoform, bearing an extended N-term domain, has been demonstrated in breast carcinoma cells<sup>24</sup> and at least three other protein-coding splice variants can be predicted by the Ensembl automatic gene annotation system ([http://www.ensembl.org/Homo\\_sapiens/Transcript/Summary?db=core;g=ENSG0000010671;r=X:101349447-101386224;t=ENST00000621635](http://www.ensembl.org/Homo_sapiens/Transcript/Summary?db=core;g=ENSG0000010671;r=X:101349447-101386224;t=ENST00000621635)). However, this is the first time that the expression of an isoform lacking most of the PH domain is found (Figure 1). By binding phosphatidylinositol-3-kinase-generated phosphatidylinositol-3,4,5-trisphosphate, PH domain allows BTK translocation to the plasma membrane and its activation.<sup>2</sup> Several other proteins have been reported to interact with BTK via the PH domain, most of them negative regulators: protein kinase C-β binding interferes

with plasma membrane targeting and subsequent activation of BTK,<sup>25,26</sup> inhibitor of BTK physically associates with BTK and downregulates its kinase activity;<sup>27,28</sup> the peptidyl-prolyl cis-trans isomerase Pin1, by binding to S21 and S115, leads to the destabilization of the protein.<sup>29</sup> It is therefore likely that because

of the absence of most of the PH domain, p65BTK would be regulated/activated differently than p77BTK, as well as be involved in different signalling pathways. Moreover, lacking the region responsible for its negative regulation, it may be expected that p65BTK would be abundantly expressed and activated. Indeed, at



variance with p77BTK, p65BTK is endowed with a strong transforming activity (Figure 4). The transforming potential of BTK has been matter of debate since its discovery and has never been completely resolved. It has been demonstrated that gain-of-function mutations introduced experimentally in the PH domain provide BTK with transforming potential;<sup>2,5-7</sup> however, no constitutively active BTK mutants have been identified so far in hematopoietic neoplasias, although it has been extensively shown that p77 plays pro-survival and anti-apoptotic roles in B cells.<sup>2,3</sup> Recently, a 80-kDa isoform, bearing an extended N-term, has been identified by Eifert *et al.*<sup>24</sup> in breast carcinoma cells having, similar to p77BTK, pro-survival and anti-apoptotic roles. As for the transforming potential of BTK, our results clearly indicate that overexpression of p77BTK is not transforming, whereas overexpression of p65BTK is even more powerful than H-RASV12 in transforming NIH-3T3 cells (Figures 4c and d). We therefore conclude that BTK is indeed an oncogene, being its transforming activity carried out by the p65, but not the p77, isoform.

A main point of the paper is that p65BTK expression and oncogenicity result from RAS/ERK pathway activation (Figure 6). Several lines of evidence demonstrate that p65BTK (over) expression is controlled, via hnRNPK, by the RAS/ERK pathway. p65BTK mRNA-bound hnRNPK is phosphorylated on Ser284 (Figure 2e), a residue known to be phosphorylated by ERK1/2.<sup>12,13</sup> Accordingly, upon blocking ERK1/2 activation p65BTK levels decreased concomitantly to hnRNPK-p-Ser284 reduction (Figure 2f). Notably, ERK1/2-mediated Ser284 phosphorylation leads to the relocalization of hnRNPK from the nucleus to the cytoplasm<sup>12</sup> and a cytoplasmic localization is necessary for hnRNPK to participate in p65BTK mRNA translation. In addition, p65BTK-mediated transformation is suppressed in the presence of CI-1040 but resumes when the inhibitor is removed from the medium (Figure 4d), consistent with a restart of ERK/hnRNPK-mediated translation of p65BTK mRNA. Accordingly, also blocking the RAS/ERK pathway upstream of ERK1/2, that is, by inhibiting endogenous RAS either by use of a chemical inhibitor or a RAS-DN, abolished p65BTK-mediated transformation of NIH-3T3 cells (Figure 4d and Supplementary Figure 5b). Even though it has been demonstrated that overexpression of wild-type RAS, at variance with mutated RAS, does not transform NIH3T3 cells,<sup>20-23</sup> a p65BTK-mediated increase in endogenous RAS levels may enhance p65BTK transforming activity by triggering a positive feedback loop. A possibility might be that p65BTK directly, or via one or more effector(s), induces RAS expression or blocks its degradation: such a mechanism would justify the stronger transforming activity of p65BTK compared with H-RASV12. Additional studies are required to ascertain this hypothesis. Conversely, p65BTK inhibition (Figure 4d) also prevented H-RASV12-mediated transformation, indicating that p65BTK is a

pivotal downstream effector of RAS and confirming that its transforming activity depends on the RAS/ERK pathway. Finally, we showed in paired peritumoural/tumoural samples from colon carcinoma patients that p65BTK expression parallels ERK1/2 activation and abnormal hnRNPK cytoplasmic localization (Figure 4e). A further indication that p65BTK is key effector in the RAS/ERK pathway is given by the results obtained on its inhibition in colon cancer cells. It is well known that the RAS/ERK pathway is critical for transducing mitogenic signals and regulating cell proliferation.<sup>30</sup> Accordingly, p65BTK inhibition profoundly affects proliferation and clonogenicity of all colon cancer cells tested (Figure 5). Given that deregulation of the RAS/ERK pathway<sup>31</sup> occurs at high frequency in colon cancers, our data indicate that p65BTK might be a novel promising therapeutic target in this kind of tumours.

A comprehensive analysis of the mammalian transcriptome showed that most genes allow the expression of alternative 5'UTRs resulting either by use of multiple transcriptional start sites or by differential splicing.<sup>32</sup> Alternative 5'UTRs may allow transcript isoforms to bind different RNA-binding proteins, thus leading to tissue-specific or stage-specific expression.<sup>33</sup> Moreover, inappropriate expression of alternative 5'UTRs can contribute to tumorigenesis as in case of alternative 5'UTRs regulating the translation of BRCA1, MDM2 and transforming growth factor- $\beta$ .<sup>32</sup> All the examples reported so far in the literature show that tissue-specific, stage-specific or inappropriate expression of transcripts bearing alternative 5'UTRs control the expression of the same CDS, making it subject to developmental, physiological or pathological regulation. Our results demonstrate for the first time that alternative 5'UTRs can contribute to the diversification of gene expression by also driving the production of different protein isoforms, endowed with different functions.

Several oncogenic proteins can be translated by both cap-dependent and IRES-dependent mechanisms, the latter being switched on to maintain the expression of specific proteins during pathological situations when cap-dependent translation is compromised.<sup>34</sup> Interestingly, p65BTK translation is strictly IRES dependent (Figures 3b and c), suggesting that its expression should be very low in physiological conditions or in nontransformed cells. Moreover, in the 5'UTR of p65BTK mRNA, three upstream ORFs are present (Supplementary Figure S2a) that, in unstressed conditions, reduce the efficiency of translation initiation of the main downstream ORF.<sup>35</sup> Indeed, basal levels of p65BTK are low in immortalized NIH-3T3 cells (Figure 4a) and very low or undetectable in peritumoural samples (Figures 1b and 4e and Supplementary Figure S6). Translational control is a crucial component of cancer development and progression, and a role for RAS/ERK signalling pathway in the regulation of cap-dependent translation via its action on mammalian target of rapamycin

**Figure 4.** p65BTK is a novel oncogenic protein acting downstream of RAS/MAPK pathway and is overexpressed in colon cancers. **(a)** NIH3T3 cells transfected with empty vector or plasmids encoding p65BTK, p77 or mutated H-RAS (H-RASV12). p65BTK expression was assessed by p65BTK-specific polyclonal antibody BN49, whereas p77BTK was probed with a monoclonal antibody against the N-term of BTK (BD). **(b)** Phase contrast images of NIH3T3 transfected with empty vector or plasmids expressing p77BTK, p65BTK, H-RASV12;  $\times 40$  magnification. To note, p77BTK-transfected NIH3T3 maintain the same appearance of the empty vector-transfected untransformed fibroblasts, whereas p65BTK-transfected NIH3T3 are similar to H-RASV12-transformed fibroblasts. **(c)** In soft agar assay, p65BTK-transfected NIH3T3 fibroblasts showed a colony-forming activity higher than H-RASV12-transfected ones ( $\times 10$  magnification). Right: number of colonies (mean of three separate wells). **(d)** Focus assay of NIH3T3 cells transfected with empty vector, H-RASV12, p65BTK or p77BTK expression plasmids, grown in the absence or presence of BTK (Ibrutinib), RAS (FTI-277) or MEK1/2 (CI-1040) inhibitors; parallel samples of p65BTK-transfected cells were treated for 16 days with CI1040 or treated for 10 days with CI1040 followed by 6 days without drug; ( $\times 10$  magnification). **(e)** Immunohistochemical detection of p65BTK, hnRNPK and p-ERK-1/2 in formalin-fixed, paraffin-embedded specimens ( $\times 40$  magnification); tumour samples (T) showing predominant cytoplasmic hnRNPK expression and moderate to strong p-ERK-1/2 levels expressed the highest amounts of p65BTK, whereas low expression of p65BTK was detectable in peritumoural (PT) samples, in which hnRNPK was exclusively or predominantly nuclear and p-ERK-1/2 levels were very low. **(f, g)** Overexpression of p65BTK in patients with stage II colon cancer. Tissue microarray (TMA) analysis of p65BTK expression was performed in tumoural/peritumoural pairs of specimens from a cohort of 83 patients and results were grouped by comparing the expression in tumoural vs peritumoural tissues **(f)** and by the intensity of the staining in the tumour tissue **(g)**.

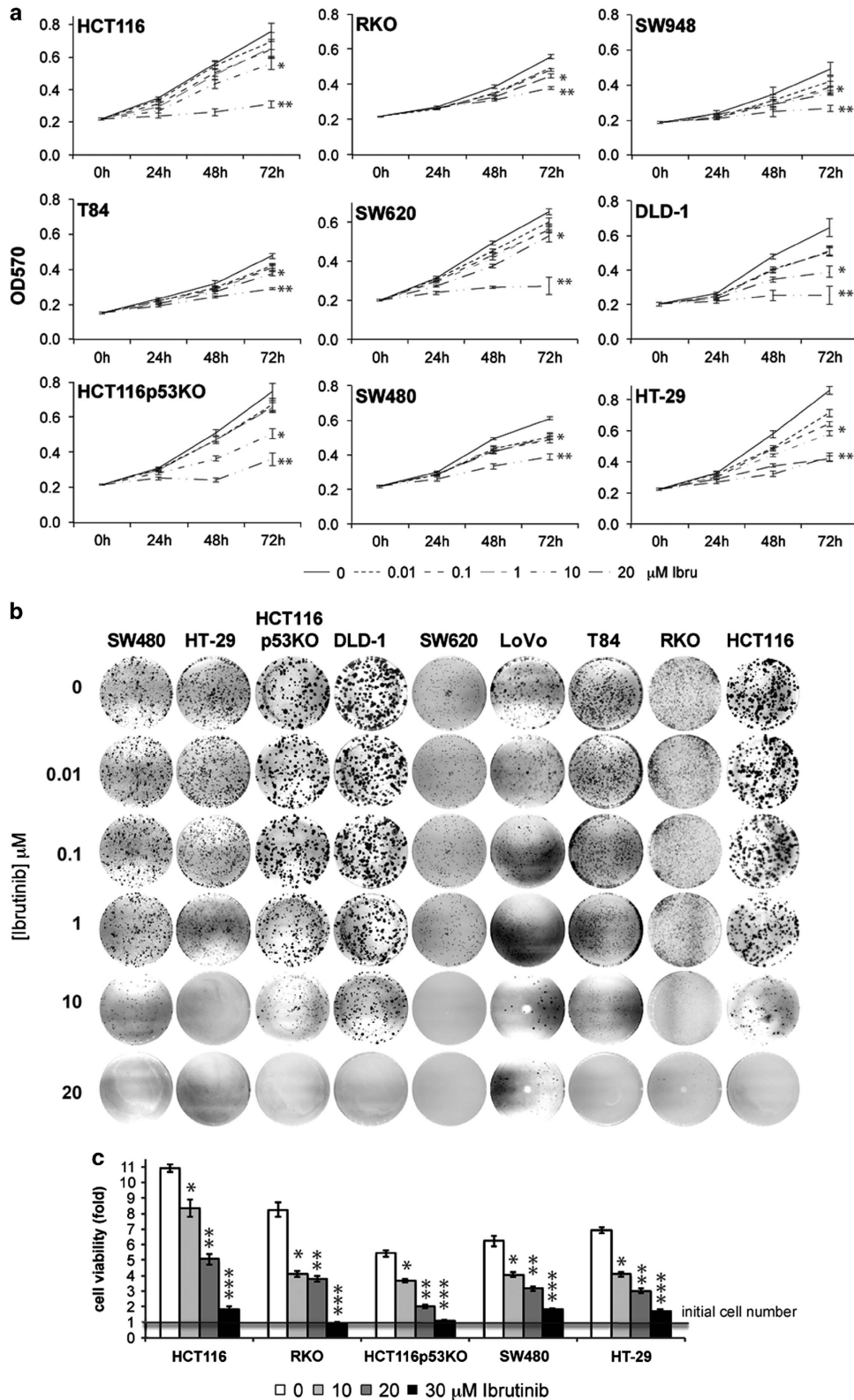


**Figure 5.** p5BTK inhibition affects growth and survival of colon cancer cells. **(a)** Time course showing Ibrutinib dose response (0, 0.01, 0.1, 1, 10, 20 μM Ibru) of colon carcinoma cell lines characterized by different genetic background; cell proliferation was determined every 24 h by MTT assay on cells incubated with Ibrutinib at the indicated concentrations; error bars show s.e.m.; data are the average of 3–5 independent experiments. Ibrutinib at 10 and 20 μM significantly decreases cell growth in all cell lines \*10 vs 0 μM Ibru:  $P < 0.05$ ; \*\*20 vs 0 μM Ibru:  $P < 0.005$ . **(b)** Clonogenicity was assessed by seeding cells at low density and incubating them with the indicated doses of Ibrutinib for 10–12 days, at the end of which colonies were stained by crystal violet. **(c)** Cell viability was assessed after 72 h of treatment with the indicated concentration of Ibrutinib; crystal violet assay was performed to quantify viable cells; data are presented as fold change of the initial cell number obtained from 3 independent experiments; error bars show s.e.m. \*10 vs 0 μM Ibru:  $P < 0.05$ ; \*\*20 vs 0 μM Ibru:  $P < 0.005$ ; \*\*\*30 vs 0 μM Ibru:  $P < 0.0005$ .



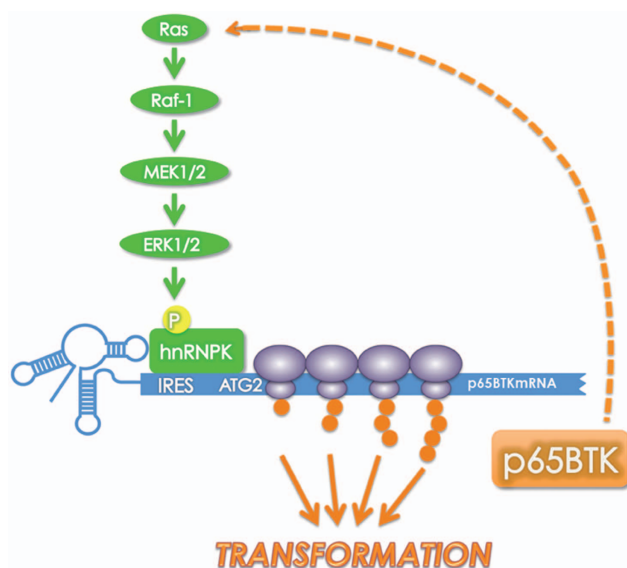


**Figure 6.** Proposed model of p65BTK regulation.

complex 1 is well accepted.<sup>36</sup> Our data about ERK/hnRNPK-dependent regulation of IRES-driven translation of p65BTK, together with the demonstration that RAS-induced transformation requires p65BTK, suggest that RAS/ERK signalling, via hnRNPK, may also play a crucial role in the regulation of IRES-dependent translation and that dysregulation of IRES-mediated translation may be a feature of cancer cells with an hyperactive RAS/ERK pathway (like colon cancer cells).

In conclusion, we show that a novel isoform of BTK is expressed outside of the hematopoietic compartment as a result of a complex post-transcriptional mechanism, and we provide evidence that alternative 5'UTRs can contribute to the diversification of gene expression by driving the production of different protein isoforms, endowed with different transforming potential. Moreover, our results demonstrating that BTK is a potent oncoprotein acting downstream of the RAS/ERK pathway, together with those showing that its inhibition profoundly affects colon cancer cells proliferation and survival, suggest that p65BTK might be a novel promising therapeutic target in colon cancer, where deregulation of the RAS/ERK pathway occurs at a very high frequency.

## MATERIALS AND METHODS

### Plasmids

Standard cloning methods were used to generate all plasmids, whereas 5' RACE was performed to clone 5' end of p65BTK mRNA. Detailed methods are described in the Supplementary Methods.

### Cell lines, culture and treatments

Isogenic p53wt (HCT116) and p53KO (HCT116p53KO) HCT116 colon carcinoma cell lines were from Dr Bert Vogelstein (Johns Hopkins University, Baltimore, MD, USA) through the GRCF Biorepository & Cell Center of the Johns Hopkins School of Medicine. The 293T, HeLa, DLD-1, SW480, RKO, T84, HT-29, SW948, SW620, SW48, LoVo, CaCo-2 and NIH3T3 and HeLa cells were from American Type Culture Collection (LGC Standards, Sesto San Giovanni, Italy). Nalm-6 were from Deutsche Sammlung von Mikroorganismen und Zellkulturen GmbH (Braunschweig, Germany). All the repositories guaranteed cell line identity by genotypic and phenotypic testing. Upon arrival, cells were expanded and frozen as seed stocks of first or second passage. All cells were passaged for a maximum of 6 weeks, after which new seed stocks were thawed for experimental use. All cells were grown at 37 °C in 5% CO<sub>2</sub> and were maintained as a subconfluent monolayer in McCoy medium (HCT116, HCT116p53KO, DLD-1, SW480, HT-29, SW620), Dulbecco's modified Eagle's

medium/Ham's F12 (T84), RPMI-1640 (Nalm-6, SW48, SW948), Ham's F12 (LoVo) or Dulbecco's modified Eagle's medium (NIH3T3, 293T, HeLa, RKO, Caco-2) supplemented with 10% fetal bovine serum (except for NIH3T3 cells medium, supplemented with 10% calf serum) and 1% penicillin/streptomycin; 1% nonessential amino acids was also added to RKO and Caco-2 medium. Cells were routinely checked for mycoplasma contamination each time a new stock was thawed. Media, serum and supplements were all from Invitrogen (Life Technologies Italia, Monza, Italy) except for calf serum (Colorado Serum Company, Denver, CO, USA). Ibrutinib and AVL-292 (Selleckchem, Houston, TX, USA) were dissolved in dimethyl sulfoxide and stored in aliquots at -80 °C.

### Transfection and silencing experiments

The siRNA and plasmid transfections were performed using Lipofectamine 2000 (Invitrogen) according to the manufacturer's instructions. Silencing experiments and siRNA sequences are described in detail in Supplementary Information. Each transfection and silencing experiment was repeated at least three times.

### Cell transformation assays

**Focus assay.** NIH3T3 cells were seeded at 70% confluency in a 6-well plate the day before and then were transfected using Lipofectamine 2000 and 4 µg DNA/well; 36 h after transfection, cells were reseeded in triplicate in 6-well plate in the presence or absence of inhibitors of BTK (Ibrutinib, 10 µM), RAS (FTI-277, 10 µM) and MEK1/2 (CI-1040 10 µM). Inhibitors were replenished each day, whereas medium was changed every other day. After 10 days, foci were fixed and stained in 1% crystal violet, 35% ethanol. Parallel samples of p65BTK-transfected cells were treated for 16 days with CI1040 or treated for 10 days with CI1040 followed by 6 days without drug.

**Soft agar assay.** An aliquot (1000 cells) of NIH3T3 cells transfected as above were resuspended in warm (37 °C) 0.4% Top Agar Solution and seeded on a solidified 0.8% Base Agar Solution, both prepared according to the protocol of the Cell Transformation Detection Assay (Merck-Millipore, Vimodrone, Italy). Cells were fed every 3 days with cell culture medium and colonies counted after 10 days by 3 independent evaluators. Cell transformation assays were repeated three times.

### Cell growth/proliferation assay

5 × 10<sup>3</sup> cells per 96-well plate were seeded in triplicate, and starting the following day (day 0) proliferation was evaluated every 24 h using a MTT-based assay (Sigma-Aldrich, Milano, Italy) according to the manufacturer's instructions. Graphs represent the average of three to five independent experiments. Average ± s.e.m. are plotted in the graphs.

### Colony assay

Cells were seeded at low density (1000 cells/well in 6-well plate) in triplicate and left untreated or treated with different concentrations of Ibrutinib. Medium (alone or containing Ibrutinib) was replaced every other day, and after 10 days colonies were fixed and stained in 1% crystal violet, 35% ethanol. Colony assays were repeated three times.

### Cell viability

Cells were seeded in sextuplicates at 70% confluency the night before and the next morning treated or not with the indicated concentrations of Ibrutinib. After 72 h, cell viability was evaluated by crystal violet staining. Briefly, after washing with phosphate-buffered saline, cells were fixed/stained with a solution of 0.5% crystal violet in 20% methanol for 20 min at room temperature and then washed extensively with tap water. Colour was extracted by adding 0.1 M acetic acid and quantified by spectrophotometer at 595 nm. Graphs represent the average of three separate experiments. Average ± s.e.m. are plotted in the graphs.

### GFP/RFP fluorescence assay

Cells transfected with GFP/RFP bicistronic vectors were harvested after 36 h, fixed with 4% paraformaldehyde in phosphate-buffered saline and counterstained with DAPI (4',6-diamidino-2-phenylindole). Fluorescence microscope examination was performed using a Nikon Eclipse 80i microscope at ×60 magnification. Images were acquired using Genikon

(Nikon Instruments, Campi Bisenzio, Italy) software and processed with Adobe Photoshop. GFP/RFP fluorescence assays were repeated three times.

### Tissue samples

Permission for using tissue specimens surgically removed from patients was granted by the ethical committee of the University of Milano-Bicocca. Multiple specimens, collected from patient admitted to Desio Hospital ( $n=13$ , for patient characteristics see Supplementary Table S1), were dissected by a pathologist from matched peritumoural/normal tissues removed during surgery and either immediately frozen at  $-80^{\circ}\text{C}$  for RNA and protein analysis or routinely fixed in formalin for subsequent histological and immunohistochemistry analysis on tissue microarray. Frozen specimens were used to measure p65BTK expression by quantitative PCR after processing with RNeasy kit (Qiagen, Milano, Italy) and by western blot upon tissue lysis in RIPA buffer, as described below. In a separate analysis, tissue microarray samples from a cohort composed of 83 patients (admitted to Trieste University Hospital; for patients characteristics see Supplementary Table S1) with a clinical diagnosis of colon cancer, classified by a pathologist as stage II, were examined for p65BTK expression by immunohistochemistry.

### Immunohistochemistry

Specimens from patients admitted to Desio Hospital ( $n=13$ ) were fixed with formalin, dehydrated, diaphanized with xylene, put in paraffin and processed for tissue microarray. Slides were stained according to standard immunohistochemistry procedures with the following primary antibodies: anti-hnRNPK (sc-25373) from Santa Cruz Biotechnologies (Heidelberg, Germany); phospho-ERK (Thr202/Tyr204) (#4370) from Cell Signaling (Danvers, MA, USA); and anti-p65BTK BN49 polyclonal antibody. Slides were digitally acquired using Aperio ScanScope System (Leica Microsystems, Milano, Italy). On specimens from patients admitted to Trieste University Hospital ( $n=83$ ), p65BTK staining was graded according to an increasing intensity by blind reading by two experienced operators and classified as negative, positive and strongly positive.

### RNA extraction and RIP

RNA was isolated using an RNeasy kit (Qiagen) following the manufacturer's instructions. In RIP experiments, RNA was purified from anti-hnRNPK (ab39975, Abcam, Cambridge, UK) immunoprecipitated complex from colon cancer cell (HCT116p53KO) lysates using the Magna RIP kit (Millipore, Vimodrone, Milano, Italy) following the manufacturer's instructions. Isotype matched antibodies were used as a control. RIP experiments were repeated three times.

### PCR

End point PCR, 5'RACE PCR and real-time PCR procedures and primers are described in Supplementary Information.

### Anti-p65BTK antibody production and characterization

BN49 polyclonal antibody produced by immunizing rabbits with a GST fusion protein encompassing the first 30N-term aa of p65BTK adsorbed to nanogold.<sup>37</sup> Antisera specificity was assessed by western blot analysis on lysates from p65BTK-expressing and p65BTK-silenced cells (Supplementary Figure 1f) and used in all western blots to probe p65BTK unless differently specified. In immunocytochemistry, specificity was additionally tested using pre-immune serum, as well as by pre-absorption with corresponding synthetic peptide/s (up to  $\sim 50$  nmol/ml) on sections from cell blocks of SW480 p65BTK-expressing and p65BTK-silenced cells (Supplementary Figure 1g) and on sections from colon cancer patient tissues.

### Western blot analysis

Protein extracts were prepared using high-salt lysis buffer (Hepes 50 mM, pH 7.5, NaCl 500 mM, DTT 1 mM, EDTA 1 mM, 0.1% NP-40) supplemented with 1% protease inhibitor cocktail (Sigma-Aldrich). Then, 10–20  $\mu\text{g}$  cell and tissues lysates were separated on 10% NuPAGE gels (Invitrogen), transferred onto a nitrocellulose membrane (Invitrogen) and incubated with the following antibodies: anti-p65BTK (BN49); anti-BTK (sc-1696) anti-hnRNPK (sc-25373) from Santa Cruz Biotechnologies; anti-ERK (#9101), anti-phospho-ERK (Thr202/Tyr204) (#4370), anti-eIF4G2 (#5169) from Cell

Signaling; anti-actin (A1978), anti-vinculin (V9264), anti-phospho-hnRNPK (SAB4504229) from Sigma-Aldrich; and anti-RAS (#05-516) from Millipore. Each single blot was reprobbed with anti-actin or anti-vinculin as loading control. Images were acquired using G:BOX XT4 Chemiluminescence and Fluorescence Imaging System (Syngene, Cambridge, UK) and processed with Adobe Photoshop.

### In vitro translation

TnT Quick Coupled Transcription/Translation Systems (Promega, Milano, Italy) has been used according to the manufacturer's instructions. Briefly, 1  $\mu\text{g}$  each plasmid DNA was mixed with 12.5  $\mu\text{l}$  Master mix from the kit and 1  $\mu\text{l}$  Transcend Biotinylated tRNA (Promega). Translated products, separated on NuPAGE and blotted onto nitrocellulose, were detected by chemiluminescence upon incubation with the horseradish peroxidase/streptavidin conjugate. The *in vitro* translation experiments were repeated three times.

### Statistical analysis

The *t*-test was applied to evaluate statistically significant differences between series of samples subjected to different experimental treatments, and  $P \leq 0.05$  was considered significant.

### CONFLICT OF INTEREST

The authors declare no conflict of interest. EG, FP and AC were partly supported by BiOnSil, srl, spin-off of the University of Milano-Bicocca. BiOnSil had no part in the design and interpretation of the study or in the publication of its results.

### ACKNOWLEDGEMENTS

We thank BiOnSil, srl, spin-off of the University of Milano-Bicocca, for making available BN49 anti-p65BTK antibody in the frame of the Scientific agreement with the University of Cagliari, and Dr Elena Sacco and Dr Luca Mologni from the University of Milano-Bicocca for the gift of the RAS-DN and pS-shRAS plasmids. This work was funded by MIUR, PON01\_02782, by Ministry of Health, RF-2010-2305526 and by University of Milano-Bicocca, FAR grants to ML.

### REFERENCES

- Rawlings DJ, Saffran DC, Tsukada S, Largaespada DA, Grimaldi JC, Cohen L *et al.* Mutation of unique region of Bruton's tyrosine kinase in immunodeficient XID mice. *Science* 1993; **261**: 358–361.
- Mohamed AJ, Yu L, Bäckesjö CM, Vargas L, Faryal R, Aints A *et al.* Bruton's tyrosine kinase (Btk): function, regulation, and transformation with special emphasis on the PH domain. *Immunol Rev* 2009; **228**: 58–73.
- Novero A, Ravella PM, Chen Y, Dous G, Liu D. Ibrutinib for B cell malignancies. *Exp Hematol Oncol* 2014; **3**: 4–10.
- Feldhahn N, Río P, Soh BN, Liedtke S, Sprangers M, Klein F *et al.* Deficiency of Bruton's tyrosine kinase in B cell precursor leukaemia cells. *Proc Natl Acad Sci USA* 2005; **102**: 13266–13271.
- Li T, Tsukada S, Satterthwaite A, Havlik MH, Park H, Takatsu K *et al.* Activation of Bruton's tyrosine kinase (BTK) by a point mutation in its pleckstrin homology (PH) domain. *Immunity* 1995; **2**: 451–460.
- Park H, Wahl MI, Afar DE, Turck CW, Rawlings DJ, Tam C *et al.* Regulation of Btk function by a major autophosphorylation site within the SH3 domain. *Immunity* 1996; **4**: 515–525.
- Dingjan GM, Maas A, Nawijn MC, Smit L, Voerman JS, Grosveld F *et al.* Severe B cell deficiency and disrupted splenic architecture in transgenic mice expressing the E41K mutated form of Bruton's tyrosine kinase. *EMBO J* 1998; **17**: 5309–5320.
- Salamov AA, Nishikawa T, Swindells MB. Assessing protein coding region integrity in cDNA sequencing projects. *Bioinformatics* 1998; **14**: 384–390.
- Komar AA, Mazumder B, Merrick WC. A new framework for understanding IRES-mediated translation. *Gene* 2012; **502**: 75–86.
- Bomsztyk K, Denisenko O, Ostrowski J. hnRNP K: one protein multiple processes. *Bioessays* 2004; **26**: 629–638.
- Carpenter B, McKay M, Dundas SR, Lawrie LC, Telfer C, Murray GI. Heterogeneous nuclear ribonucleoprotein K is over expressed, aberrantly localised and is associated with poor prognosis in colorectal cancer. *Br J Cancer* 2006; **95**: 921–927.
- Habelhah H, Shah K, Huang L, Ostareck-Lederer A, Burlingame AL, Shokat KM *et al.* ERK phosphorylation drives cytoplasmic accumulation of hnRNP-K and inhibition of mRNA translation. *Nat Cell Biol* 2001; **3**: 325–330.

- 13 Notari M, Neviani P, Santhanam R, Blaser BW, Chang JS, Galletta A *et al*. A MAPK/HNRPK pathway controls BCR/ABL oncogenic potential by regulating MYC mRNA translation. *Blood* 2006; **107**: 2507–2516.
- 14 Marash L, Liberman N, Henis-Korenblit S, Sivan G, Reem E, Elroy-Stein O *et al*. DAP5 promotes cap-independent translation of Bcl-2 and CDK1 to facilitate cell survival during mitosis. *Mol Cell* 2008; **30**: 447–459.
- 15 Shi Y, Sharma A, Wu H, Lichtenstein A, Gera J. Cyclin D1 and c-myc internal ribosome entry site (IRES)-dependent translation is regulated by AKT activity and enhanced by rapamycin through a p38 MAPK- and ERK-dependent pathway. *J Biol Chem* 2005; **280**: 10964–10973.
- 16 Didiot MC, Hewett J, Varin T, Freuler F, Selinger D, Nick H *et al*. Identification of cardiac glycoside molecules as inhibitors of c-Myc IRES-mediated translation. *J Biomol Screen* 2013; **1**: 407–419.
- 17 Silvera D, Formenti SC, Schneider RJ. Translational control in cancer. *Nat Rev Cancer* 2010; **10**: 254–266.
- 18 Guha M. Imbruvica-next big drug in B-cell cancer-approved by FDA. *Nat Biotechnol* 2014; **32**: 113–115.
- 19 Burger JA. Bruton's tyrosine kinase (BTK) inhibitors in clinical trials. *Curr Hematol Malig Rep* 2014; **9**: 44–49.
- 20 Tabin CJ, Bradley SM, Bargmann CI, Weinberg RA, Papageorge AG, Scolnick EM *et al*. Mechanism of activation of a human oncogene. *Nature* 1982; **300**: 143–148.
- 21 Reddy EP, Reynolds RK, Santos E, Barbacid M. A point mutation is responsible for the acquisition of transforming properties by the T24 human bladder carcinoma oncogene. *Nature* 1982; **300**: 149–152.
- 22 Taparowsky E, Suard Y, Fasano O, Shimizu K, Goldfarb M, Wigler M. Activation of the T24 bladder carcinoma transforming gene is linked to a single amino acid change. *Nature* 1982; **300**: 762–766.
- 23 Seeburg PH, Colby WW, Capon DJ, Goeddel DV, Levinson AD. Biological properties of human c-Ha-ras1 genes mutated at codon 12. *Nature* 1984; **312**: 71–74.
- 24 Eifert C, Wang X, Kokabee L, Kourtidis A, Jain R, Gerdes MJ *et al*. A novel isoform of the B cell tyrosine kinase BTK protects breast cancer cells from apoptosis. *Gene Chrom Cancer* 2013; **52**: 961–975.
- 25 Yao L, Kawakami Y, Kawakami T. The pleckstrin homology domain of Bruton tyrosine kinase interacts with protein kinase C. *Proc Natl Acad Sci USA* 1994; **91**: 9175–9179.
- 26 Kang SW, Wahl MI, Chu J, Kitaura J, Kawakami Y, Kato RM *et al*. PKCbeta modulates antigen receptor signaling via regulation of Btk membrane localization. *EMBO J* 2001; **20**: 5692–5702.
- 27 Liu W, Quinto I, Chen X, Palmieri C, Rabin RL, Schwartz OM *et al*. Direct inhibition of Bruton's tyrosine kinase by IBtk, a Btk-binding protein. *Nat Immunol* 2001; **2**: 939–946.
- 28 Spatuzza C, Schiavone M, Di Salle E, Janda E, Sardiello M, Fiume G *et al*. Physical and functional characterization of the genetic locus of IBtk, an inhibitor of Bruton's tyrosine kinase: evidence for three protein isoforms of IBtk. *Nucleic Acids Res* 2008; **36**: 4402–4416.
- 29 Yu L, Mohamed AJ, Vargas L, Bergl f A, Finn G, Lu KP *et al*. Regulation of Bruton tyrosine kinase by the peptidylprolyl isomerase Pin1. *J Biol Chem* 2006; **281**: 18201–18207.
- 30 De Luca A, Maiello MR, D'Alessio A, Pergameno M, Normanno N. The RAS/RAF/MEK/ERK and the PI3K/AKT signalling pathways: role in cancer pathogenesis and implications for therapeutic approaches. *Expert Opin Ther Targets* 2012; **16**: S17–S27.
- 31 Fang JY, Richardson BC. The MAPK signaling pathways and colorectal cancer. *Lancet Oncol* 2005; **6**: 322–327.
- 32 Smith L. Post-transcriptional regulation of gene expression by alternative 5'-untranslated regions in carcinogenesis. *Biochem Soc Trans* 2008; **36**: 708–711.
- 33 Wurth L, Gebauer F. RNA-binding proteins, multifaceted translational regulators in cancer. *Biochim Biophys Acta* 2014; **1849**: 881–886.
- 34 Spriggs KA, Stoneley M, Bushell M, Willis AE. Re-programming of translation following cell stress allows IRES-mediated translation to predominate. *Biol Cell* 2008; **100**: 27–38.
- 35 Barbosa C, Peixeiro I, Rom o L. Gene expression regulation by upstream open reading frames and human disease. *PLoS Genet* 2013; **8**: e1003529.
- 36 Gao B, Roux PP. Translational control by oncogenic signaling pathways. *Biochim Biophys Acta* 2014; **1849**: 753–765.
- 37 Pow DV, Crook DK. Extremely high titre polyclonal antisera against small neurotransmitter molecules: rapid production, characterisation and use in light- and electron-microscopic immunocytochemistry. *J Neurosci Methods* 1993; **48**: 51–63.



This work is licensed under a Creative Commons Attribution 4.0 International License. The images or other third party material in this article are included in the article's Creative Commons license, unless indicated otherwise in the credit line; if the material is not included under the Creative Commons license, users will need to obtain permission from the license holder to reproduce the material. To view a copy of this license, visit <http://creativecommons.org/licenses/by/4.0/>

Supplementary Information accompanies this paper on the Oncogene website (<http://www.nature.com/onc>)

## SUPPLEMENTARY INFORMATIONS

### SUPPLEMENTARY METHODS

#### Plasmids

Full length p65BTK was amplified from HCT116p53KO-derived cDNA using primers #1 and #2 (see below for primers' sequences) and cloned into pGEM vector (Promega) to originate pGEM-FLp65. p65FL, the p65BTK-expressing vector was created by PCR subcloning the entire p65BTK sequence from the pGEM-FLp65 plasmid into pcDNA3.1 (Invitrogen) using primers #3 and #4. p65CDS was created by PCR subcloning the p65BTK CDS from pGEM-FLp65 plasmid with primers #5 and #6, designed to exclude the 5' and 3'UTRs. p65\_5'UTR $\Delta$ k1, p65\_5'UTR $\Delta$ k2, p65\_5'UTR $\Delta$ k3, p65\_5'UTR $\Delta$ k4 were created by PCR subcloning into pcDNA3.1 p65BTK amplified from pGEM-FLp65 using reverse primer #4 and as forward primers oligonucleotides annealing downstream of the first (primer #7), second (primer #8), third (primer #9) and fourth (primer #10) hnRNPk binding site, respectively. p65BTK\_msATG1, \_nsATG1 and \_nsATG2 were created via site-directed mutagenesis (QuikChange Site-Directed Mutagenesis Kit, Stratagene), according to manufacturer instructions'. As a template p65FL plasmid was used together with primers #11 and #12 to introduce a missense (ms) or with primers #13 and #14 to introduce a non-sense (ns) mutation into the ATG1, or with primers #15 and #16 to introduce a ns mutation into the ATG2. Full length p77BTK was amplified from Nalm6-derived cDNA using primers #1 and #17 and cloned into pGEM vector to originate pGEM-FLp77. p77FL was created by PCR subcloning the entire p77BTK sequence from the pGEM-FLp77 plasmid into pcDNA3.1 using primers #18 and #4. p77CDS was created by PCR subcloning p77BTK from pGEM-FLp77 plasmid into pcDNA3.1 with primers #19 and #6, designed to exclude the 5' and 3'UTRs. p77BTK\_msATG1 was created by introducing via site-directed mutagenesis a ms mutation into the ATG1 of p77BTK from the p77FL plasmid using primers used #10 and #11. To create the bi-cistronic vectors, Red Fluorescent Protein (RFP) and Green Fluorescent Protein (GFP) were amplified from

pDsRed2-N1 (Clontech) (primers #21 and #22) and pcDNA3.1-EGFP (Invitrogen) (primers #23 and #24), respectively, then independently subcloned into pGEM vector (pGEM-RFP and pGEM-GFP). The whole 5'UTR of p65BTK and  $\Delta k1/\Delta k2/\Delta k3/\Delta k4$ -deleted counterparts were amplified from pGEM-FLp65 (reverse primer #4 and forward primers #3, #7, #8, #9 and #10 respectively) and ligated upstream of GFP in pGEM-GFP: the resulting products were first subcloned downstream RFP in pGEM-RFP (*EcoRI/XbaI* excision), and successively the whole sequence RFP-5'UTR ( $\Delta k1/\Delta k2/\Delta k3/\Delta k4$ )-GFP was cut out (*BamHI/XbaI* digestion) and cloned into pcDNA3.1 to create RFP-UTRp65BTK-GFP, RFP-UTRp65 $\Delta k1$ -GFP, RFP-UTRp65 $\Delta k2$ -GFP, RFP-UTRp65 $\Delta k3$ -GFP, RFP-UTRp65 $\Delta k4$ -GFP, respectively. pSuper plasmids targeting BTK and H-RAS were made by inserting a 19-bp target sequence (BTK: 5'-TTTCTATGGAGTCTTCTGC-3'; H-RAS: 5'-GGCAAGAGTGCGCTGACCATC-3') in pSuper plasmid (Oligoengine) cloned in both sense and antisense orientations, separated by a loop sequence, in order to obtain the transcription of a short-hairpin RNA. pcDNA3-RAS-DN was made by subcloning RAS-DN in pcDNA3. 3-HRASV12 was from K. Helin lab. pRSV-RAS-DN and pSuperior-shRAS were kind gifts of Dr. Elena Sacco (University of Milano-Bicocca) and Dr. Luca Mologni (University of Milano-Bicocca), respectively.

#1: 5' GTAATTTTATTTTATCAAAACACCCTC 3'

#2: 5' TCTTTTGGTGGACTCTGCTACG 3'

#3: 5' GGATCCTCTTTTGGTGGACTCTGCTACG 3'

#4: 5' GTAATTTTATTTTATCAAAACACCCTC 3'

#5: 5' CTCGAGAAATGGAGCAAATTTCAATCAT 3'

#6: 5' GGGCCCGGCGAGCTCAGGATTCTTCA 3'

#7: 5' GGATCCCAGAAAAAGAAAACATCACCTCTA 3'

#8: 5' GGATCCGAGGGAAGCCAGGACTAGG 3'

#9: 5' GGATCCCGTCCCCGAGGGAAGC 3'

#10: 5' GGATCCAGATCCTCTGGCCTCCCC 3'

#11: 5'GTGAACTCCAGAAAGAAGAAGCTTTGGCCGCAGTGATTCTG 3'  
#12: 5'CAGAATCACTGCGGCCAAAGCTTCTTCTTTCTGGAGTTCAC 3'  
#13: 5' GTGAACTCCAGAAAGAAGAAGCTTAGGCCGCAGTGATTCTG 3'  
#14: 5'CAATGATTGAAATTTGCTCCTATCACTGGACTCTTCACCTC 3'  
#15: 5'GAGGTGAAGAGTCCAGTGAATAGAGCAAATTTCAATCATTG 3'  
#16: 5'CAATGATTGAAATTTGCTCTATTCCTGGACTCTTCACCTC 3'  
#17: 5' AACTGAGTGGCTGTGAAAGG 3'  
#18: 5' GGATCCAACCTGAGTGGCTGTGAAAGG 3'  
#19: 5' CTCGAGTCATGGCCGCAGTGATTCTG 3'  
#20: 5' GCGGCCGCTTCACTGGACTCTTCACCTCT 3'  
#21: 5' GGATCCACCATGGCCTCCTCCG 3'  
#22: 5' GAATTCTTAAGATCTCAGGAACAGGTGG 3'  
#23: 5' GCGGCCGCCTAGAATGGCTAGCAAAGGA 3'  
#24: 5' TCTAGATTATTTGTAGAGCTCATCCATGC 3'

**Silencing experiments.** For silencing endogenous BTK in colon cancer cell lines a mix of siRNA targeting sequences in exon 5 (nts 895-913) and exon 8 (nts: 518-536) were used. For silencing specifically p65BTK, exon 1b was targeted by using each of the following siRNAs: B1 (nts: 160-182), B2 (nts: 237-259), B3(nts: 179-197). For silencing specifically p77BTK, exon 1a was targeted by using siRNA for a sequence between nts 78-100. For silencing exogenous overexpressed p65BTK in 293T cells, the combination of B1, B2 and B3 siRNAs was used. For silencing hnRNPK in colon cancer cell lines a mix of 3 different siRNA (s6737, s6738, s6739 Silencer® Select from Invitrogen) was used. Luciferase siRNAs (Luciferase GL2) were from Eurofins MWG Operon. In all silencing experiments cells were harvested and lysed 48 hs after the silencing, protein extracts were separated on 10% NuPAGE gels and western blotted as described below.

exon 5: 5'GGGAAAGAAGGAGGTTTCA 3'

exon 8: 5'GAAGCTTAAAACCTGGGAG 3'

B1: 5'GAACACCTTTTCGCAGCAAAGT 3'

B2: 5' GCCAGTTGGTCCATTCAACAAAT 3'

B3: 5' ACTGCTAATTCAATGAAGA 3'

exon 1a: 5'CAGTGTCTGCTGCGATCGAGTCC 3'

**PCR. Endpoint PCR.** Purified RNA was retrotranscribed using SuperScript VILO cDNA Synthesis kit (Invitrogen). To identify the BTK isoform expressed in colon cancer cell lines amplification was performed using 200 ng cDNA and 0.4  $\mu$ M of the following primers, covering the entire coding sequence (CDS) of BTK (NM\_000062). cDNA from NALM-6 was used as a control.

1F: 5' CTCAGA CTGTCCTTCCTCTC 3'

8R: 5'GTTGCTTTCCTCCAAGATAAAAT 3'

2F: 5'ATCCCAACAGAAAAAGAAAACAT 3'

8F: 5'ATCTTGAAAAAGCCACTACCG 3'

14F: 5'CTCAAATATCCAGTGTCTCAACA 3'

12F: 5'TGATACGTCATTATGTTGTGTGTT 3'

14R: 5'ATCATGACTTTGGCTTCTTCAAT 3'

17R: 5'CTTTAACAACCTCCTTGATCGTTT 3'

19R: 5'TCAGGATTCTTCATCCATGACATCTA 3'

HeLa cDNA was amplified as above using the following primers, targeting the RPF/GFP sequence:

RED-F : 5' GACATCCCCGACTACAAGAAG 3'

GFP-R: 5' GAAAGGGCAGATTGTGTGCG 3'

PCR products were separated on 1% gel and visualized upon ethidium bromide staining.

*5'RACE.* Amplification of 5' end of p65BTK mRNA was performed using the 5' RACE System for Rapid Amplification of cDNA Ends from Invitrogen, following manufacturer's instructions. For 5' end identification RNA extracted from colon cancer cell lines was used. PCR products were ligated in pGEM-T easy vector (Promega) and 10 clones/each cell line were sequenced by using T7/Sp6 primers (Eurofins MWG Operon).

*Real-time PCR.* To quantify p65BTK mRNA immunoprecipitated in RIP experiments cDNA was synthesized using a High Capacity RNA to cDNA Master Mix and analysed by quantitative PCR (qPCR) using customized TaqMan gene expression assays on a 7900HT Real-Time PCR system (all Applied Biosystems). Amplification specific for p65BTK isoform was performed using the following primers:

p65FW: 5' CCCATTATGTGGCAGGCACT 3'

p65REV: 5'CTTCAGAAAGATGCTCTCCAGA 3'

p65PROBE: 5' TGA ACTCCAGAAAGAAGAA 3'

p65BTK gene expression was normalized to phosphoglycerate kinase expression (#Hs99999906\_m1, Applied Biosystem), and expressed as fold-change of control samples.





cancer cells. (c) cDNA retro-transcribed from RNAs extracted from colon and lymphoid cancer cells, was PCR amplified using a forward primer annealing in exon 1b and a reverse primer annealing on the second common exon. (d) colon cancer-derived mRNA contains a first exon (exon 1b) different from the one expressed in B cells (exon 1a). ClustalW alignment of p77BTK (NM\_000061) with p65BTK sequence identified by 5'RACE PCR in colon cancer cell lines. Only the alignment of the exon 1 and the first 50 nucleotides of exon 2 are shown. (e) BLAST alignment of the first 5 exons from p77BTK cDNA (NM\_000061) and p65BTK cDNA vs. genomic DNA. (f) Characterization of BN49 polyclonal antibodies. *Left*: Western blot analysis of lysates from colon cancer cells (Co: HCT116) transfected with control (luc) or p65BTK-specific siRNA and harvested after 48hs. Lysates from lymphoid leukemia cells (Ly: Nalm6) were used as controls expressing p77BTK. Bovine serum albumin (BSA, MW 66 kDa) was used as MW marker. Bound antibodies were revealed using a chemiluminescent system. *Right*: The same blot was re-incubated with a monoclonal antibody raised against the PH domain-containing N-term of p77BTK (# 611117 BD Transduction laboratories) and therefore not reacting with p65BTK: immunoreactivity was revealed using a fluorescent secondary antibody (AlexaFluor488, Molecular Probes). (g) Top: Western blot analysis of lysates from SW480 colon cancer cells harvested 48hs after transfection with control (luc) or p65BTK-specific siRNA and used to produce cells blocks. Bottom: IHC using BN49 on slides from cells blocks.

**a** UCCC putative hnRNP binding sites

UCAACAAAUG upstream Open Reading Frames (uORFs)

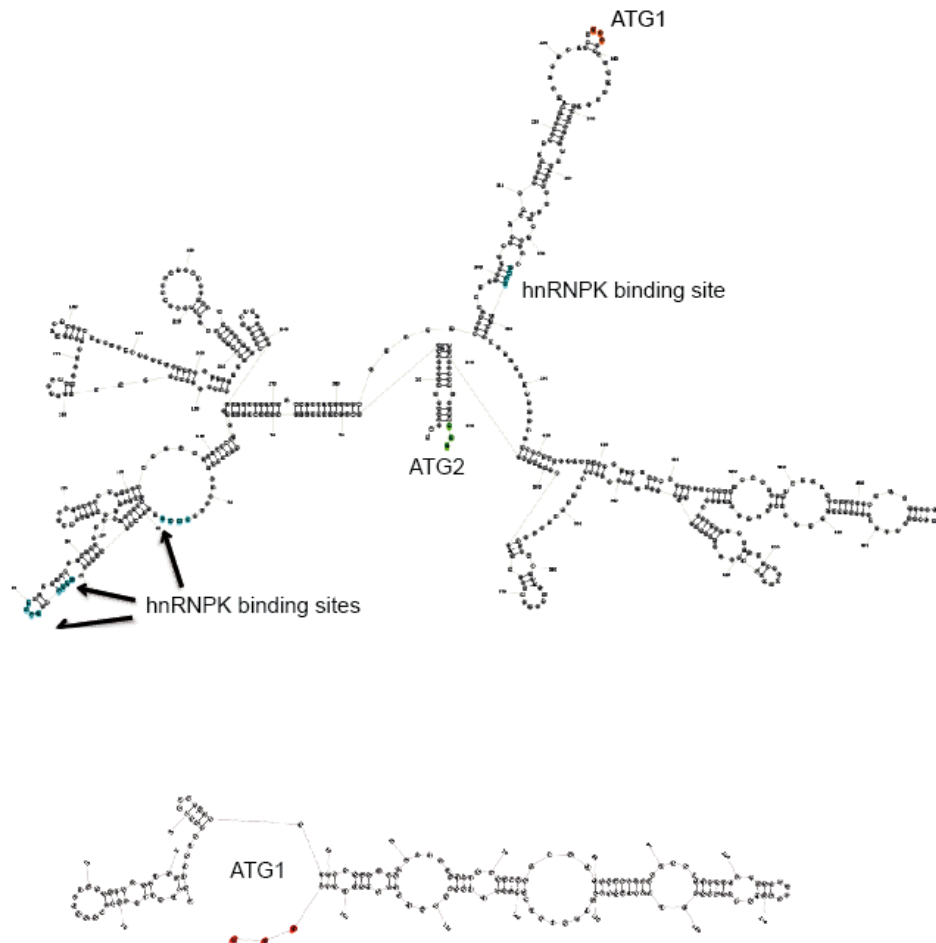
AUG start of translation in p77BTK (*GCUAUGGCC* italic underlined letters surrounding the starting codon indicate the Kozak consensus sequence)

AUG start of translation in p65BTK

**p65 whole 5'UTR**

```
UCUUUUGGUGGACUCUGCUACGUAUGGGCCUUCACUGAAGGGAGCAGUCUUUUUCCCAGAUCCUCUGGCCUCCCCUCCCCGAGGC
AAGCCAGGACUAGG GUCGAAUGAAGGGGUCCACCUCACGUVUCCAUVCCUGUCCACCUCAGGUCACUGGGAACCCUUUCG
CAGCAAACUGCUAAUUAUGAAGACCUGGAGGGAGCCAAUUGUUCAGUUCUUAUCACAUGGCCAGUUGGUCCAUAACAACAA
UGGUUAUUGGAUGCCAUUAUGUGGCAGGCACUGUUCGGGGGAGAGCACACAGGUGAACUCCAGAAAGAAGAAGCUAUGGCCGCA
GUGAUUCUGGAGAGCAUCUUUCUGAAGCGAUCCCAACAGAAAAAGAAAACAUCACCUCUAAACUUAAGAAGCGCCUGUUUCUU
GACCGUGCACAAAACUCUCCUACUAUGAGUAUGACUUUGAACUGGGGAGAAGAGGCAGUAAGAAGGGUCAAUAGAUGUUGAGAAGA
UCACUUGUGUUGAAACAGUGGUUCCUGAAAAAAAUCCUCCUCCAGAAAGACAGAUUCCGAGAAGAGGUGAAGAGUCCAGUGAA AUG
```

**b**



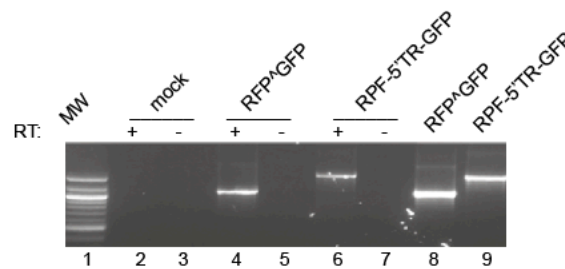
**Supplementary Figure 2. hnRNP sites in p65BTK-encoding mRNA.** (a) Bioinformatics' analysis of the 5'UTR of p65BTK messenger showing four putative hnRNP binding sites. (b) 5'UTR sequences from p65BTK-encoding and p77BTK-encoding mRNAs were analysed and compared using AveRNA application from the RNAsoft package (<http://www.masoft.ca>) and the structures visualized by the VARNAv3-7.jar application ([fr.orsay.lri.varna.applications.VARNAGUI](http://fr.orsay.lri.varna.applications.VARNAGUI)). ATG1, ATG2 and hnRNP binding sites are indicated. *Top*: 5'UTR structure of the mRNA encoding p65BTK. *Bottom*: 5'UTR structure of the mRNA encoding p77BTK.

**a** <http://iresite.org/>

Sequences producing significant alignments:	Score (bits)	E Value
<a href="#">IRESite Id:110</a> Apaf-1 gene	29	3.1
<a href="#">IRESite Id:223</a> UtrA gene	28	10
<a href="#">IRESite Id:140</a> EMCV-R virus	28	10
<a href="#">IRESite Id:465</a> plasmid pUTRA/CAT with functional UtrA IRES from ...	28	10
<a href="#">IRESite Id:238</a> plasmid pbetaGAL/UtrA/CAT with functional UtrA IR...	28	10
<a href="#">IRESite Id:239</a> plasmid (deltaCMV)betaGAL/UtrA/CAT with functiona...	28	10
<a href="#">IRESite Id:437</a> RhPV IGR virus	26	35
<a href="#">IRESite Id:437</a> RhPV_5NCR virus	26	35
<a href="#">IRESite Id:59</a> PSIV_IGR virus	26	35
<a href="#">IRESite Id:68</a> idfix virus	26	35
<a href="#">IRESite Id:491</a> AQP4 gene	26	35

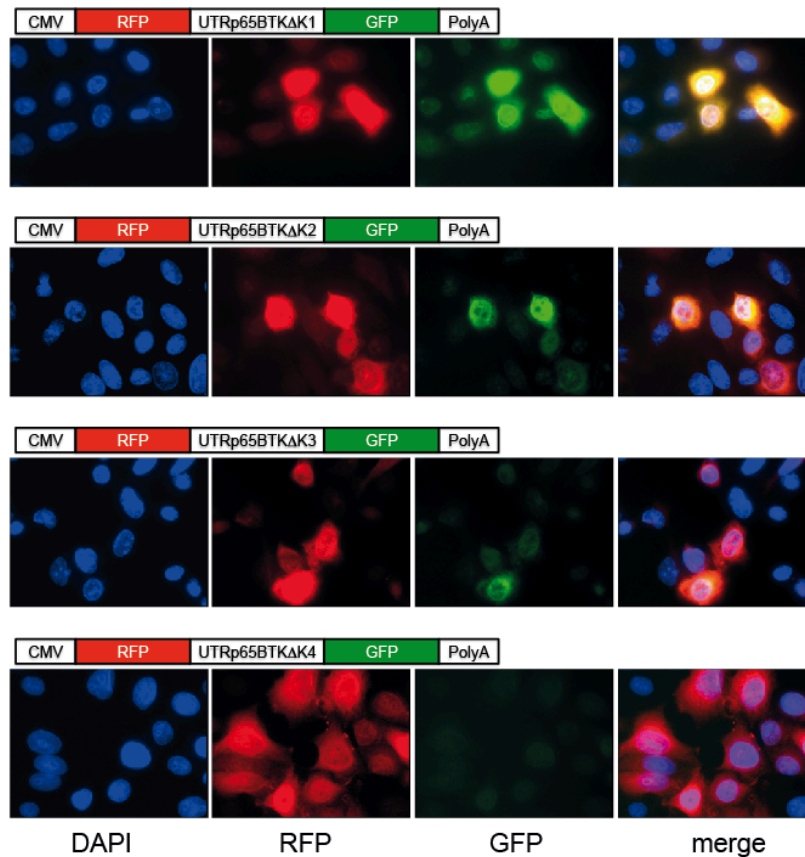
Sequences producing significant alignments:	Score (bits)	E Value
<a href="#">IRESite Id:59</a> 2D structure of transcript of PSIV_IGR virus	23	1.2
<a href="#">IRESite Id:140</a> 2D structure of transcript of EMCV-R virus	21	3.9
<a href="#">IRESite Id:35</a> 2D structure of transcript of c-myc gene	21	3.9
<a href="#">IRESite Id:597</a> 2D structure of transcript of TMEV virus	19	13
<a href="#">IRESite Id:222</a> 2D structure of transcript of HCV_type_1a virus	19	13
<a href="#">IRESite Id:222</a> 2D structure of transcript of HCV_type_1a virus	19	13
<a href="#">IRESite Id:222</a> 2D structure of transcript of HCV_type_1a virus	19	13
<a href="#">IRESite Id:42</a> 2D structure of transcript of HAV_HM175 virus	19	13
<a href="#">IRESite Id:42</a> 2D structure of transcript of HAV_HM175 virus	19	13
<a href="#">IRESite Id:519</a> 2D structure of transcript of FGF1A gene	19	13
<a href="#">IRESite Id:225</a> 2D structure of transcript of CVB3 virus	19	13
<a href="#">IRESite Id:491</a> 2D structure of transcript of AQP4 gene	19	13
<a href="#">IRESite Id:359</a> 2D structure of transcript of plasmid pXLCSEFV1-44...	19	13
<a href="#">IRESite Id:482</a> 2D structure of transcript of plasmid pRKMI2F wit...	19	13
<a href="#">IRESite Id:481</a> 2D structure of transcript of plasmid pRKMI1F wit...	19	13
<a href="#">IRESite Id:541</a> 2D structure of transcript of plasmid pBiCAQP4 wi...	19	13
<a href="#">IRESite Id:109</a> 2D structure of transcript of XIAP_305-466 gene	17	44
<a href="#">IRESite Id:109</a> 2D structure of transcript of XIAP_5-464 gene	17	44
<a href="#">IRESite Id:471</a> 2D structure of transcript of MYB gene	17	44
<a href="#">IRESite Id:486</a> 2D structure of transcript of plasmid pbetaGAL/5'...	17	44

**c**

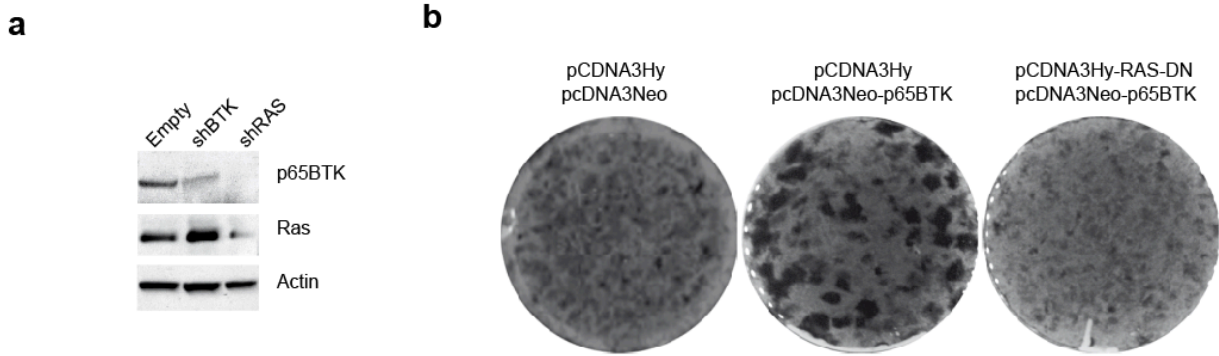


**Supplementary Figure 3. 5'UTR of p65BTK mRNA contain an IRES but not a cryptic promoter.** (a, b) The putative IRES sequence in the 5'UTR of p65BTK mRNA was identified by searching against the IRESite database (<http://www.iresite.org>) for sequences producing significant alignments. List of sequences producing significant alignment as (a) a linear sequence and (b) a secondary structure. (c) The presence of a cryptic promoter was ruled out by verifying that a unique messenger coding for both RFP and GFP is transcribed in transfected cells. cDNA from HeLa cells upon mock transfection (mock) or transfection with a bi-cistronic vector encoding CMV-regulated RFP and promoterless-GFP (RFP<sup>GFP</sup>) or GFP under the control of p65BTK 5'UTR (RFP-5'UTR-GFP) was amplified using a forward primer annealing in the RFP sequence and a reverse primer annealing in the GFP sequence. Products of the retro-transcription reaction in absence (RT -: lanes 3, 5, 7) or presence of reverse transcriptase (RT +: lanes 2, 4, 6) followed by PCR amplification were visualized in 1% agarose gel. PCR products, amplified using RFP<sup>GFP</sup>

and RFP-5'UTR-GFP plasmids as templates, loaded in lane 8 and 9, respectively, showed the same size of the products obtained using as templates the cDNA from the cells transfected with the correspondent plasmids.

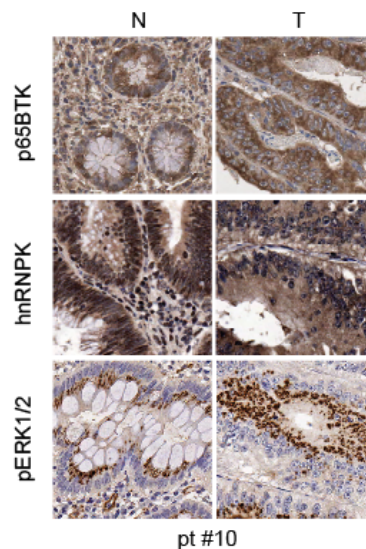


**Supplementary Figure 4. IRES-dependent translation of p65BTK depends on hnRNPk.** Fluorescence of HeLa cells upon transfection with progressive deletion mutants lacking: the first hnRNPk binding sites present in the 5'UTR of p65BTK mRNA ( $\Delta K1$ ) (first row); the first and the second hnRNPk binding sites present in the 5'UTR of p65BTK mRNA ( $\Delta K2$ ) (second row); the first, the second and the third hnRNPk binding sites present in the 5'UTR of p65BTK mRNA ( $\Delta K3$ ) (third row); all four ( $\Delta K4$ ) hnRNPk binding sites present in the 5'UTR of p65BTK mRNA (fourth row). DAPI was used to stain nuclei.



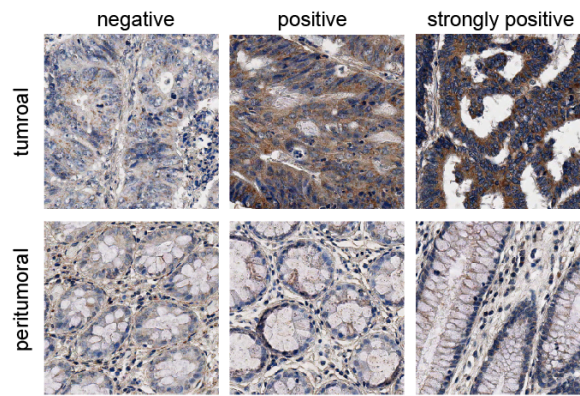
**Supplementary Figure 5. p65BTK and RAS expression and transforming activities.**

(a) NIH3T3 cells transfected with empty vector or plasmids encoding shBTK, and shRAS, tested 48 after transfection. (b) Focus assay of NIH3T3 cells stably transfected with empty vectors and RASV-DN, and then transiently transfected with p65BTK expression plasmid. Plates were stained with crystal violet 2 weeks after transfection.

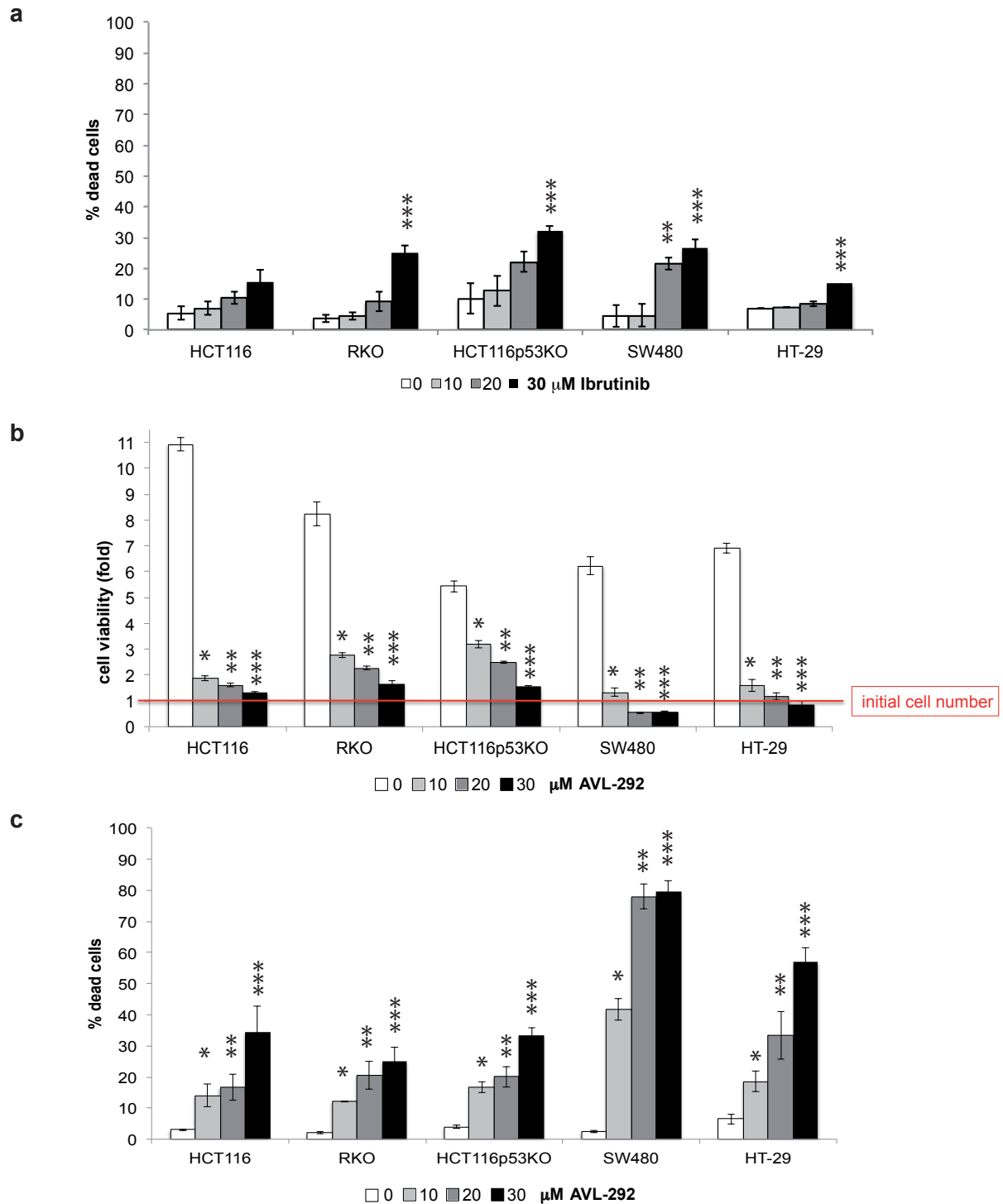


**Supplementary Figure 6. p65BTK expression, cytoplasmic hnRNPk accumulation and ERKs activation.**

Immunohistochemical detection of p65BTK, hnRNPk and pERK1/2 in formalin-fixed paraffin-embedded specimens. p65BTK staining was performed by using BN49 polyclonal antibody, counterstaining with Haematoxylin and Eosin. 40x magnification. A single peritumoural sample with very high p65BTK expression shows also intense cytoplasmic hnRNPk staining and high pERK1/2 activation.



**Supplementary Figure 7. p65BTK expression in colon cancers.** Examples of p65BTK staining, graded accordingly to an increasing intensity by blind reading by 2 experienced operators. p65BTK staining was performed by using BN49 polyclonal antibody, counterstaining with Haematoxylin and Eosin. 40x magnification.



**Supplementary Figure 8. BTK inhibitor AVL-292 exerts a stronger effect on growth and survival of colon cancer cells than Ibrutinib.**

(a) Cell death was assessed after 72 hs treatment with the indicated concentrations of Ibrutinib by Trypan blue staining. Data are the average from 3 independent experiments; error bars show SEM. \*\*\* 30 μM vs 0 μM Ibru:  $p < 0.05$ ; \*\* 20 μM vs 0 μM Ibru:  $p < 0.05$ . (b) Cell viability was assessed after 72 hs treatment with the indicated concentration of AVL-292; crystal violet assay was performed to quantify viable cells; data is presented as fold change of the initial cell number obtained from three independent experiments; error bars show SEM. \* 10 μM vs 0 μM Ibru:  $p < 0.05$ ; \*\* 20 μM vs 0 μM Ibru:  $p < 0.05$ ; \*\*\* 30 μM vs 0 μM Ibru:  $p < 0.05$ . (c) Cell



death was assessed after 72 hs treatment with the indicated concentrations of AVL-292 by Trypan blue staining. Data are the average from 3 independent experiments; error bars show SEM. \* 10  $\mu$ M vs 0  $\mu$ M Ibru:  $p < 0.05$ ; \*\* 20  $\mu$ M vs 0  $\mu$ M Ibru:  $p < 0.05$ ; \*\*\* 30  $\mu$ M vs 0  $\mu$ M Ibru:  $p < 0.05$ .

Patients from Desio Hospital							
	sex	age	diagnosis	grade	stage	lymph nodes	metastasis
#1	F	59	villous adenoma	0	in situ	0	0
#2	M	73	adenoca	3	III	3	0
#3	M	80	adenoca	2	II	0	0
#4	M	78	adenoca	2	II	1	0
#5	M	82	adenoca	1	II	0	0
#6	M	59	adenoca	3	III	0	liver, peritoneum
#7	M	78	adenoca	2	II	0	0
#8	M	67	adenoca	2	III	1	liver
#9	M	70	adenoca	3	II	0	0
#10	F	90	adenoca	1	II	0	0
#11	M	74	adenoca	2	IV	1	liver
#12	F	51	adenoca	2	II	1	0
#13	M	55	adenoca	3	III	1	0

Patients from Trieste cohort							
	sex	age	diagnosis	grade	stage	lymph nodes	metastasis
#1	M	72	adenoca	1	II	0	0
#3	F	59	adenoca	2	II	0	0
#5	M	72	adenoca	2	II	0	0
#7	M	63	adenoca	2	II	0	0
#9	M	64	adenoca	2	II	0	0
#11	M	70	adenoca	1	II	0	0
#13	F	63	adenoca	2	II	0	0
#15	F	69	adenoca	1	II	0	0
#17	M	69	adenoca	2	II	0	0
#19	M	68	adenoca	2	II	0	0
#21	F	56	adenoca	2	II	0	0
#23	F	46	adenoca	2	II	0	0
#25	F	77	adenoca	2	II	0	0
#27	F	59	adenoca	2	II	0	0
#29	M	60	adenoca	2	II	0	0
#31	F	67	adenoca	2	II	0	0
#33	M	61	adenoca	2	II	0	0
#35	F	67	adenoca	2	II	0	0
#37	M	73	adenoca	2	II	0	0
#39	M	81	adenoca	2	II	0	0
#41	M	66	adenoca	2	II	0	0
#43	M	76	adenoca	2	II	0	0
#45	F	76	adenoca	1	II	0	0
#47	F	61	adenoca	2	II	0	0
#49	F	68	adenoca	2	II	0	0
#51	F	72	adenoca	1	II	0	0
#53	F	80	adenoca	2	II	0	0
#55	M	84	adenoca	2	II	0	0
#57	F	71	adenoca	2	II	0	0
#59	M	82	adenoca	2	II	0	0
#61	M	72	adenoca	2	II	0	0
#63	F	59	adenoca	2	II	0	0
#65	M	54	adenoca	2	II	0	0
#67	F	66	adenoca	1	II	0	0
#69	M	59	adenoca	2	II	0	0
#71	M	65	adenoca	2	II	0	0
#73	M	64	adenoca	2	II	0	0
#75	M	69	adenoca	2	II	0	0
#77	M	79	adenoca	2	II	0	0
#79	M	58	adenoca	2	II	0	0
#81	F	56	adenoca	2	II	0	0
#83	M	58	adenoca	2	II	0	0

**Supplementary Table 1.** Patients characterization. In the table are shown: age, sex, diagnosis, TNM classification and grade.

